

Feedback control of surface roughness in sputtering processes using the stochastic Kuramoto–Sivashinsky equation

Yiming Lou, Panagiotis D. Christofides*

*Department of Chemical Engineering, University of California, 405 Hilgard Avenue,
Box 951592, Los Angeles, CA 90095-1592, USA*

Available online 6 November 2004

Abstract

This work focuses on control of surface roughness in sputtering processes including two surface micro-processes, diffusion and erosion. The fluctuation of surface height of such sputtering processes can be described by the stochastic Kuramoto–Sivashinsky equation (KSE), a fourth-order stochastic partial differential equation (PDE). Specifically, we consider sputtering processes, including surface diffusion and erosion, on a one-dimensional lattice and design feedback controllers based on stochastic PDEs to regulate the surface roughness at desired levels. We initially reformulate the stochastic KSE into a system of infinite stochastic ordinary differential equations (ODEs) by using modal decomposition. A finite-dimensional approximation of the stochastic KSE is then derived that captures the dominant mode contribution to the surface roughness. A state feedback controller is designed based on the finite-dimensional approximation to control the surface roughness. Feedback control of surface roughness in three different sputtering processes with different sputtering yield functions and different ratios of erosion and diffusion rates is subsequently studied. Kinetic Monte-Carlo simulations are first performed to simulate the evolution of the surface height fluctuation in the three sputtering processes. Then, a systematic identification approach is used to identify the parameters of the stochastic KSE models describing the sputtering processes by using the data from kinetic Monte-Carlo simulations. Specifically, the evolution of state covariance of the stochastic KSE models is directly obtained from multiple kinetic Monte-Carlo simulation runs. The correlations between model parameters and the state covariance of the stochastic KSE models are established and the parameters of the stochastic KSE models are subsequently computed by using least-mean-square fitting so that the evolution of the surface roughness computed from the stochastic KSE models is consistent with that computed from kinetic Monte-Carlo simulations. Feedback controllers are designed and applied to kinetic Monte-Carlo models of the sputtering processes to control the surface roughness to desired levels.

© 2004 Elsevier Ltd. All rights reserved.

Keywords: Feedback control; Sputtering processes; Surface roughness; Stochastic Kuramoto–Sivashinsky equation

1. Introduction

Sputtering processes are widely used in the thin film and semiconductor fabrication to remove material from the surface of solids through the impact of energetic particles. In many cases sputtering is used to smooth out surface features. The surface morphology of thin films after the sputter erosion strongly depends on conditions such as incident ion energy, sputtered substrate temperature and material composition (Makeev, Cuerno, & Barabasi, 2002b). The surface roughness of thin films of advanced materials is an important

variable to control because it strongly affects the quality of such films. Due to the increasingly stringent requirements on the quality of such films, feedback control of surface roughness of sputtering processes becomes important.

In a sputtering process, the surface is directly shaped by the microscopic surface processes (e.g., erosion, diffusion and surface reaction), which are stochastic processes. Therefore, the stochastic nature of sputtering processes must be fully considered in the modeling and control of the surface roughness of such processes. The desire to understand and control the thin film micro-structure has motivated extensive research on fundamental mathematical models describing the microscopic features of surfaces formed by surface micro-processes, which include (1)

* Corresponding author. Tel.: +1 310 794 1015; fax: +1 310 206 4107.
E-mail address: pdcs@seas.ucla.edu (P.D. Christofides).

kinetic Monte-Carlo methods (e.g., Chen, Bogaerts, Depla, & Ignatova, 2003; Fichtorn, & Weinberg, 1991; Gillespie, 1976; Gilmer, Huang, de la Rubia, Torre, & Baumann, 2000; Kersch, Morokoff, & Werner, 1994; Reese, Raimondeau, & Vlachos, 2001; Shitara et al., 1992); and (2) stochastic partial differential equations (PDEs) (e.g., Cuerno, Makse, Tomasone, Harrington, & Stanley, 1995; Edwards & Wilkinson, 1982; Lauritsen, Cuerno, & Makse, 1996; Villain, 1991; Vvedensky, Zangwill, Luse, & Wilby, 1993). Furthermore, the study of feedback control of surface roughness is also motivated by the possibility to obtain roughness measurements in real-time using scanning tunneling microscopy (Voigtländer, 2001), spectroscopic ellipsometry techniques (Zapfen, Messier, & Collin, 2001), grazing-incidence small-angle X-ray scattering (GISAXS) (Renaud et al., 2003) or by combination of on-line measurement techniques for measuring gas phase compositions with off-line measurement techniques for measuring surface roughness. An implementation of the latter approach was recently reported in Ni et al. (2004), where it was used to measure carbon composition of thin films in plasma-enhanced chemical vapor deposition using combination of optical emission spectroscopy (OES) and X-ray photoelectron spectroscopy (XPS).

The kinetic Monte-Carlo simulation methods can be used to predict average properties of thin films (which are of interest from a control point of view, for example, surface roughness), by explicitly accounting for the micro-processes that directly shape thin film microstructure. At this point, it is important to note that in the present paper we work exclusively with lattice kinetic Monte-Carlo methods as opposed to equilibrium continuous-space Monte-Carlo methods. Recently, a methodology for feedback control of surface roughness using kinetic Monte-Carlo models has been developed in Lou and Christofides (2003a, 2003b). The methodology leads to the design of (a) real-time roughness estimators by using multiple small lattice kinetic Monte-Carlo simulators, adaptive filters and measurement error compensators; and (b) feedback controllers based on the real-time roughness estimators. The method was successfully applied to control surface roughness in a *GaAs* deposition process using an experimentally determined kinetic Monte-Carlo process model (Lou & Christofides, 2004a). Moreover, kinetic Monte-Carlo methods have also been used to study the dynamics of complex deposition processes including multiple components with both short-range and long-range interactions and to perform predictive control design to control final surface roughness (Ni & Christofides, 2004).

Recently, an equation-free time-stepper-based control methodology was developed for processes described by atomistic rules (e.g., kinetic Monte-Carlo, Molecular Dynamics, Brownian Dynamics), and for which explicit, evolution equations at the macroscopic level are not available in closed form (Makeev, Maroudas, & Kevrekidis, 2002). The method circumvents the problem of closed-form process model unavailability by using “coarse” time-steppers, which are microscopic-scale simulators, to predict evolution

of the process variables over macroscopic time and space scales through “coarse” projective integration. The method was used to control both spatially lumped systems described by kinetic Monte-Carlo simulations (Siettos, Armaou, Makeev, & Kevrekidis, 2003) and spatially distributed processes (Armaou, Siettos, & Kevrekidis, 2004).

However, the fact that kMC models are not available in closed-form makes very difficult to use them for system-level analysis and the design and implementation of real-time model-based control systems. Although the “coarse” time-stepper based approach allows controller design using linear control theory to control “coarse-variables” which are low statistical moments of the microscopic distributions (e.g., surface coverage, the zeroth moment of adspecies distribution on a lattice), to control higher statistical moments of the microscopic distributions, such as the surface roughness (the second moment of height distribution on a lattice), linear deterministic models may not be sufficient, because the effect of the stochastic nature of the microscopic processes becomes very significant and must be addressed both in the model construction and controller design. For many deposition and sputtering processes, closed-form process models, in the form of stochastic PDEs, can be derived based on the microscopic rules and the corresponding master equation (e.g., Cuerno et al., 1995; Edwards & Wilkinson, 1982; Lauritsen et al., 1996; Villain, 1991; Vvedensky et al., 1993). To achieve better closed-loop performance, it is desirable to design feedback controllers on the basis of process models. This has motivated recent research on the development of a method for feedback control of surface roughness based on stochastic PDE process models (Lou & Christofides, 2004b). This method involves reformulation of the stochastic PDE into a system of infinite stochastic ordinary differential equations by using modal decomposition, derivation of a finite-dimensional approximation that captures the dominant mode contribution to the surface roughness, and state feedback controller design based on the finite-dimensional approximation.

Both the deterministic and the stochastic Kuramoto–Sivashinsky equation (KSE) are important PDEs which describe a variety of chemical and physical processes. Some examples of processes that are described by the deterministic KSE are falling liquid films (Chen & Chang, 1986), unstable flame fronts (Sivashinsky, 1977) and interfacial instabilities between two viscous fluids (Hooper & Grimshaw, 1985). Analytical and numerical studies of the dynamics of the deterministic KSE have revealed that the dominant dynamics of the KSE can be adequately characterized by a small number of degrees of freedom (e.g., Temam, 1988). This has motivated extensive research focusing on the design of linear/nonlinear finite-dimensional output feedback controllers (Armaou & Christofides, 2000a, 2000b) for stabilization of the zero solution of the KSE on the basis of ordinary differential equation (ODE) approximations, obtained through linear (Armaou & Christofides, 2000a) and nonlinear (Armaou & Christofides, 2000b) Galerkin’s method, that accurately describe the dominant dynamics of the KSE for a given value of

the instability parameter. The global stabilization of the KSE has also been addressed via distributed static output feedback control (Christofides & Armaou, 2000). A nonlinear boundary feedback controller was also proposed in Liu and Krstić (2001) that enhances the rate of convergence to the spatially uniform steady-state of the KSE, for values of the instability parameter for which this steady state is open-loop stable. The issue of optimal actuator/sensor placement for the KSE was also addressed in Lou and Christofides (2003c) so that the desired control objectives are achieved with minimal energy use.

The stochastic KSE can be used to model the evolution of the height profile for surfaces in a variety of sputtering processes including surface erosion by ion sputtering (Cuerno et al., 1995; Lauritsen et al., 1996), surface smoothing by energetic clusters (Insepop, Yamada, & Sosnowski, 1997) and ZrO₂ thin film growth by reactive ion beam sputtering (Qi et al., 2003). The long-time behavior of the stochastic KSE was studied through renormalization-group analysis (Cuerno & Lauritsen, 1995) and its numerical solution was obtained in Drotar, Zhao, Lu, and Wang (1999). The problem of the existence and uniqueness of the solution to the stochastic KSE was also investigated in Duan and Ervin (2001). Even though the above works have led to fundamental understanding of the physical meaning of the various terms and mathematical properties of the stochastic KSE, the problem of feedback controller design for systems described by the stochastic KSE has not been addressed.

This work focuses on control of surface roughness in sputtering processes including two surface micro-processes, diffusion and erosion. The fluctuation of surface height of such sputtering processes can be described by the stochastic KSE, a fourth-order stochastic PDE. Specifically, we consider sputtering processes, including surface diffusion and erosion, on a one-dimensional lattice and use the method proposed in Lou and Christofides (2004b) to design a feedback controller to regulate the surface roughness at a desired level. We initially reformulate the stochastic KSE into a system of infinite stochastic ordinary differential equations (ODEs) by using modal decomposition. A finite-dimensional approximation of the stochastic KSE is then derived that captures the dominant mode contribution to the surface roughness. A state feedback controller is designed based on the finite-dimensional approximation to control the surface roughness. Feedback control of surface roughness in three different sputtering processes with different sputtering yield functions and different ratios of erosion and diffusion rates is subsequently studied. Kinetic Monte-Carlo simulations are first performed to simulate the evolution of the surface height fluctuation in the three sputtering processes. Then, a systematic identification approach is used to identify the parameters of the stochastic KSE models describing the sputtering processes by using the data from kinetic Monte-Carlo simulations. Specifically, the evolution of state covariance of the stochastic KSE models is directly obtained from multiple kinetic Monte-Carlo simulation runs. The correlations between model parameters and

the state covariance of the stochastic KSE models are established and the parameters of the stochastic KSE models are subsequently computed by using least-mean-square fitting so that the evolution of the surface roughness computed from the stochastic KSE models is consistent with that computed from kinetic Monte-Carlo simulations. Feedback controllers are designed and applied to kinetic Monte-Carlo models of the sputtering processes to control the surface roughness to desired levels.

2. Preliminaries

2.1. Process description

We consider a 1D-lattice representation of a crystalline surface in a sputtering process, which includes two surface micro-processes, erosion and diffusion. The solid-on-solid assumption is made which means that no defects or overhangs are allowed in the process (Siegert & Plischke, 1994). The microscopic rules are as follows: a site, i , is first randomly picked among the sites of the whole lattice and the particle at the top of this site is subject to: (a) erosion with probability f ; or (b) diffusion with probability $1 - f$.

If the particle at the top of site i is subject to erosion, the particle is removed from the site i with probability $P_e Y(\phi_i)$. P_e is determined as $\frac{1}{7}$ times the number of occupied sites in a box of size 3×3 centered at the site i , which is shown in Fig. 1. There is a total of nine sites in the box. The central one is the particle to be considered for erosion (the one marked by filled circle). Among the remaining eight sites, the site above the central site of interest must be vacant since the central site is a surface site. Therefore, only seven of the eight sites can be occupied and the maximum value of P_e is 1. $Y(\phi_i)$ is the sputtering yield function defined as follows:

$$Y(\phi_i) = y_0 + y_1 \phi_i^2 + y_2 \phi_i^4 \quad (1)$$

where y_0 , y_1 and y_2 are process dependent constants (see Section 4 for different values of y_0 , y_1 and y_2 in different sputtering processes) and ϕ_i is the local slope defined as fol-

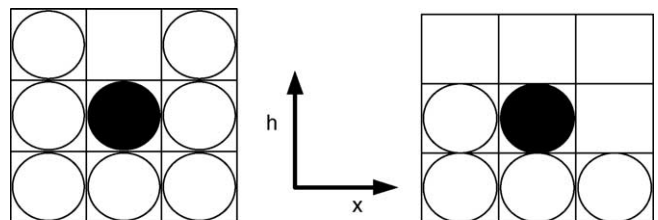


Fig. 1. Schematic of the rule to determine P_e . P_e is defined as $\frac{1}{7}$ times the number of occupied sites in a box of size 3×3 centered at the particle on the top of site i ; $P_e = 1$ in the left figure and $P_e = \frac{4}{7}$ in the right figure, where the particle marked by filled circle is on the top of site i .

lows:

$$\phi_i = \tan^{-1} \left(\frac{h_{i+1} - h_{i-1}}{2a} \right) \quad (2)$$

where a is the lattice parameter and h_{i+1} and h_{i-1} are the values of surface height at sites $i + 1$ and $i - 1$, respectively.

If the particle at the top of site i is subject to diffusion, one of its two nearest neighbors, j ($j = i + 1$ or $i - 1$) is randomly chosen and the particle is moved to the nearest neighbor column with probability $w_{i \rightarrow j}$ as follows:

$$w_{i \rightarrow j} = \frac{1}{1 + \exp(\beta \Delta H_{i \rightarrow j})} \quad (3)$$

where $\Delta H_{i \rightarrow j}$ is the energy difference between the final and initial states of the move, $\beta = 1/k_B T$ and H is defined through the Hamiltonian of an unrestricted solid-on-solid model as follows (Siegert & Plischke, 1994):

$$H = \left(\frac{J}{a^2} \right) \sum_{k=1}^L (h_k - h_{k+1})^n \quad (4)$$

where J is the bond energy, L is the total number of sites in the lattice and n is a positive number. In the simulations carried out in this work, we use $n = 2$. With this definition of H , there is a positive Schwoebel barrier (Schwoebel, 1969) for particles to diffuse in downhill direction. When a particle approaches a step from the upper terrace, it has to create a double step at the step edge. Since the energy of a double step is larger than the energy of two single steps, the diffusion particle is repelled from the down step and is preferable to diffuse in uphill direction (Siegert & Plischke, 1994).

Remark 1. Note that the term “erosion”, in general, is used to capture a variety of surface phenomena including desorption, etching, or physical sputtering from the surface. In this study, we focus on surface erosion due to physical sputtering processes. Also, we note that a full-scale model of a sputtering process would consist of a 2D-lattice representation of the surface. We reduce the dimensionality by considering a 1D-lattice representation of the surface in this work to simplify our development, but the developed feedback control method can be applied to control surface roughness in sputtering processes taking place on two-dimensional surfaces (see the discussion in Remark 5).

2.2. Stochastic PDE model of the sputtering process

The sputtering process is a stochastic process. Kinetic Monte-Carlo simulation can be used to predict the evolution of the surface configuration in this process. The kinetic Monte-Carlo model is a first-principle model in the sense that the erosion rules are explicitly considered in the model. Mathematically, kinetic Monte-Carlo simulation methods provide an unbiased realization of the master equation (Gillespie, 1976; Van Kampen, 1992), which describes the evolution of the probability that the surface is at a certain configuration.

Kinetic Monte-Carlo simulation can predict average properties of the surface of a sputtering process (which are of interest from a control point of view, for example, surface roughness). Since a kinetic Monte-Carlo simulation run constitutes a realization of a stochastic process, simulation results from a large number of different simulation runs are not identical. However, by averaging the results from different simulation runs, the averaged properties of the surface converge to the values obtained from the solution of the master equation.

Kinetic Monte-Carlo models are not available in closed-form, which makes very difficult to perform model-based control design on the basis of kinetic Monte-Carlo models. As an alternative, closed-form stochastic PDE models can be derived based on the erosion rules to describe the evolution of the surface configuration in a way that is consistent to that predicted by kinetic Monte-Carlo models. In this work, we focus on model-based feedback control design for surface roughness control using a stochastic PDE model of the sputtering process under consideration. The equation for the height fluctuations of the surface in this sputtering process was derived in (Lauritsen et al., 1996) and is a stochastic Kuramoto–Sivashinsky equation of the following form:

$$\frac{\partial h}{\partial t} = -v \frac{\partial^2 h}{\partial x^2} - \kappa \frac{\partial^4 h}{\partial x^4} + \frac{\lambda}{2} \left(\frac{\partial h}{\partial x} \right)^2 + \xi(x, t) \quad (5)$$

where $x \in [-\pi, \pi]$ is the spatial coordinate, t is the time, $h(x, t)$ is the height of the surface at position x and time t , v and κ are two constants, and $\xi(x, t)$ is a Gaussian noise with zero mean and covariance:

$$\langle \xi(x, t) \xi(x', t') \rangle = \sigma^2 \delta(x - x') \delta(t - t') \quad (6)$$

where σ is a constant, $\delta(\cdot)$ is the dirac function, and $\langle \cdot \rangle$ denotes the expected value. Note that the noise covariance depends on both space x and time t . We note that this stochastic KSE representation for the surface morphological evolution in sputtering processes is limited to surface morphologies that do not involve re-entrant features (which is a property that holds for the sputtering process described in Section 2.1); the re-entrant features could arise under certain sputtering conditions and are catastrophic for the surface.

The surface roughness, r , is represented by the standard deviation of the surface from its average height and is computed as follows:

$$r(t) = \sqrt{\frac{1}{2\pi} \int_{-\pi}^{\pi} [h(x, t) - \bar{h}(t)]^2 dx} \quad (7)$$

where $\bar{h}(t) = 1/2\pi \int_{-\pi}^{\pi} h(x, t) dx$ is the average surface height.

The height–height correlation function is also commonly used to measure surface roughness (e.g., Palasantzas, 1993; Tejedor, Šmilauer, Roberts, & Joyce, 1999). When the height–height correlation function is used, the surface roughness follows a power-law dependence on the lateral separation up to a certain value denoted as the critical length and

saturates when the lateral separation is larger than the critical length (Palasantzas, 1993; Sinha, Sirota, Garoff, & Stanley, 1988). When the surface roughness is defined as the standard deviation of the surface from its average height as in Eq. (7), it is independent of the simulation lattice size (Kalke & Baxter, 2001), provided that the lattice size is sufficiently large. Since in this study, we will compare our simulation results from the solution of stochastic KSE and that from kinetic Monte-Carlo simulations, we use Eq. (7) to measure the surface roughness.

Our objective is to control the surface roughness of the sputtering process to a desired level. In the process model of Eq. (5), the second-order-derivative term is the linearization of the surface curvature within the small-slope approximation and the fourth-order-derivative term originates from the surface diffusion rule of Eqs. (3) and (4) (Lauritsen et al., 1996). The inclusion of the nonlinear term $\lambda/2(\nabla h)^2$ in a general model for interface evolution with both growth and corrosion processes was first justified in Kardar, Parisi, and Zhang (1986) by considering the growth of an Eden cluster. In the specific sputtering processes considered in this study, the nonlinear term $\lambda/2(\partial h/\partial x)^2$ corresponds to the effect of $Y(\phi)$ on the surface fluctuations, which is a nonlinear function of the local slope; we note that the nonlinearities become more significant in the model of Eq. (5) at the late stage of the evolution of the surface when large slopes develop (Cuerno et al., 1995). In this work, we focus on the problem of feedback control of the sputtering process using linearizations of the stochastic KSE with appropriately identified parameters.

To proceed, we formulate the linearized KSE with distributed control in the spatial domain $[-\pi, \pi]$ as follows:

$$\frac{\partial h}{\partial t} = -\nu \frac{\partial^2 h}{\partial x^2} - \kappa \frac{\partial^4 h}{\partial x^4} + \sum_{i=1}^p b_i(x)u_i(t) + \xi(x, t) \quad (8)$$

subject to periodic boundary conditions:

$$\frac{\partial^j h}{\partial x^j}(-\pi, t) = \frac{\partial^j h}{\partial x^j}(\pi, t), \quad j = 0, \dots, 3 \quad (9)$$

and the initial condition:

$$h(x, 0) = h_0(x) \quad (10)$$

where u_i is the i th manipulated input, p is the number of manipulated inputs and b_i is the i th actuator distribution function (i.e., b_i determines how the control action computed by the i th control actuator, u_i , is distributed (e.g., point or distributed actuation) in the spatial interval $[-\pi, \pi]$).

To study the dynamics of Eq. (8), we initially consider the eigenvalue problem of the linear operator of Eq. (8), which takes the form:

$$\begin{aligned} A\bar{\phi}_n(x) &= -\nu \frac{d^2 \bar{\phi}_n(x)}{dx^2} - \kappa \frac{d^4 \bar{\phi}_n(x)}{dx^4} \\ &= \lambda_n \bar{\phi}_n(x), \quad n = 1, \dots, \infty, \quad (11) \\ \frac{d^j \bar{\phi}_n}{dx^j}(-\pi) &= \frac{d^j \bar{\phi}_n}{dx^j}(\pi), \quad j = 0, \dots, 3 \end{aligned}$$

where λ_n denotes an eigenvalue and $\bar{\phi}_n$ denotes an eigenfunction. A direct computation of the solution of the above eigenvalue problem yields $\lambda_0 = 0$ with $\psi_0 = 1/\sqrt{2\pi}$, and $\lambda_n = \nu n^2 - \kappa n^4$ (λ_n is an eigenvalue of multiplicity two) with eigenfunctions $\phi_n = (1/\sqrt{\pi}) \sin(nx)$ and $\psi_n = (1/\sqrt{\pi}) \cos(nx)$ for $n = 1, \dots, \infty$. From the solution of the eigenvalue problem shown in Eq. (11), it follows that for fixed values of $\nu > 0$ and $\kappa > 0$, the number of unstable eigenvalues of A is finite and the distance between two consecutive eigenvalues (i.e., λ_n and λ_{n+1}) increases as n increases. Furthermore, the eigenspectrum of the operator A in Eq. (11), $\sigma(A)$ can be partitioned as $\sigma(A) = \sigma_1(A) \cup \sigma_2(A)$, where $\sigma_1(A)$ contains the first m (with m finite) eigenvalues (i.e., $\sigma_1(A) = \{\lambda_1, \dots, \lambda_m\}$) and $\sigma_2(A)$ contains the remaining eigenvalues (i.e., $\sigma_2(A) = \{\lambda_{m+1}, \dots, \}$).

To present the method that we use to design a feedback controller on the basis of the stochastic KSE of Eq. (8), we first derive stochastic ODE approximations of Eq. (8) using modal decomposition. To this end, we first expand the solution of Eq. (8) in an infinite series in terms of the eigenfunctions of the operator of Eq. (11) as follows:

$$h(x, t) = \sum_{n=1}^{\infty} \alpha_n(t)\phi_n(x) + \sum_{n=0}^{\infty} \beta_n(t)\psi_n(x) \quad (12)$$

where $\alpha_n(t)$, $\beta_n(t)$ are time-varying coefficients. Substituting the above expansion for the solution, $h(x, t)$, into Eq. (8) and taking the inner product with the adjoint eigenfunctions, $\phi_n^*(z) = (1/\sqrt{\pi}) \sin(nz)$ and $\psi_n^*(z) = (1/\sqrt{\pi}) \cos(nz)$, the following system of infinite stochastic ODEs is obtained:

$$\begin{aligned} \frac{d\alpha_n}{dt} &= (\nu n^2 - \kappa n^4)\alpha_n \\ &+ \sum_{i=1}^p b_{i\alpha_n} u_i(t) + \xi_\alpha^n(t) \\ \frac{d\beta_n}{dt} &= (\nu n^2 - \kappa n^4)\beta_n \\ &+ \sum_{i=1}^p b_{i\beta_n} u_i(t) + \xi_\beta^n(t); \quad n = 1, \dots, \infty \end{aligned} \quad (13)$$

where

$$\begin{aligned} b_{i\alpha_n} &= \int_{-\pi}^{\pi} \phi_n(x)b_i(x)dx, \quad b_{i\beta_n} = \int_{-\pi}^{\pi} \psi_n(x)b_i(x)dx \\ \xi_\alpha^n(t) &= \int_{-\pi}^{\pi} \xi(x, t)\phi_n(x)dx, \quad \xi_\beta^n(t) = \int_{-\pi}^{\pi} \xi(x, t)\psi_n(x)dx \end{aligned} \quad (14)$$

The covariances of $\xi_\alpha^n(t)$ and $\xi_\beta^n(t)$ can be computed by using the following result (Åström, 1970):

Result 1. If (1) $f(x)$ is a deterministic function; (2) $\eta(x)$ is a random variable with $\langle \eta(x) \rangle = 0$ and covariance $\langle \eta(x)\eta(x') \rangle = \sigma^2 \delta(x - x')$; and (3) $\epsilon = \int_a^b f(x)\eta(x)dx$, then

ϵ is a random number with $\langle \epsilon \rangle = 0$ and covariance $\langle \epsilon^2 \rangle = \sigma^2 \int_a^b f^2(x) dx$.

Using **Result 1**, we obtain $\langle \xi_\alpha^n(t) \xi_\alpha^n(t') \rangle = \sigma^2 \delta(t - t')$ and $\langle \xi_\beta^n(t) \xi_\beta^n(t') \rangle = \sigma^2 \delta(t - t')$.

In this work, the controlled variable is the expected value of surface roughness, $\sqrt{\langle r^2 \rangle}$. According to Eq. (12), we have $\bar{h}(t) = \beta_0(t) \psi_0$. Therefore, $\sqrt{\langle r^2 \rangle}$ can be rewritten in terms of α_n and β_n as follows:

$$\begin{aligned} \sqrt{\langle r^2 \rangle} &= \sqrt{\frac{1}{2\pi} \left\langle \int_{-\pi}^{\pi} (h(x, t) - \bar{h}(t))^2 dx \right\rangle} \\ &= \sqrt{\frac{1}{2\pi} \left\langle \int_{-\pi}^{\pi} \sum_{i=1}^{\infty} [\alpha_i(t)^2 \phi_i(x)^2 + \beta_i(t)^2 \psi_i(x)^2] dx \right\rangle} \\ &= \sqrt{\frac{1}{2\pi} \left\langle \sum_{i=1}^{\infty} (\alpha_i^2 + \beta_i^2) \right\rangle} \\ &= \sqrt{\frac{1}{2\pi} \sum_{i=1}^{\infty} [\langle \alpha_i^2 \rangle + \langle \beta_i^2 \rangle]} \end{aligned} \tag{15}$$

Therefore, the surface roughness control problem for the stochastic KSE system of Eq. (8) is formulated as the one of controlling the covariance of the states α_n and β_n of the system of infinite stochastic ODEs of Eq. (13).

Remark 2. While the parameters of stochastic PDE models for many deposition processes and sputtering processes can be derived based on the corresponding master equations, which describe the evolution of the probability that the surface is at a certain configuration (see, for example, Lauritsen et al., 1996; Vvedensky, 2003); for all practical purposes, the stochastic PDE model parameters should be identified by matching the prediction of the stochastic PDE model to that of kinetic Monte-Carlo simulations (see Ni & Christofides, 2005 for a method to construct stochastic PDE models using kinetic Monte-Carlo simulation). The reason for this is the two assumptions which are made in the derivation of the stochastic PDE models from the master equation. Specifically, if $\mathbf{H} = \{h_1, h_2, \dots\}$ represents the surface configuration, $\mathbf{r} = \{r_1, r_2, \dots\}$ is the array of jump lengths at each site and $W(\mathbf{H}; \mathbf{r})$ is the transition rate from \mathbf{H} to $\mathbf{H} + \mathbf{r}$, it is assumed that there exists a positive real number δ such that (1) $W(\mathbf{H}; \mathbf{r}) \approx 0$, for $|\mathbf{r}| > \delta$; and (2) $W(\mathbf{H} + \Delta\mathbf{H}; \mathbf{r}) \approx W(\mathbf{H}; \mathbf{r})$, for $|\Delta\mathbf{H}| < \delta$ (Van Kampen, 1992). Because the difference in successive configurations is one height unit on a single site, the first assumption can be satisfied by increasing the number of lattice sites in the deposition process (equivalently, reducing the size of a single lattice on a fixed spatial domain as considered in this work). However, due to the dependence of the final deposition site on the local surface configuration, a change in a surface site by one height unit can produce a step change in W , which violates the second assumption; increasing the number of

sites in the deposition process cannot alleviate this problem (Haselwandter & Vvedensky, 2002). Therefore, increase of the lattice sites can reduce the error between the solution of the stochastic PDE and that of the kinetic Monte-Carlo simulation due to the first assumption, however, it cannot completely eliminate the model error between the expected roughness value obtained from the discrete microscopic kinetic Monte-Carlo simulation and from the stochastic PDE (which is a continuous approximation of the discrete process) due to the fact that the second assumption cannot be fully satisfied. As a result, to design feedback controllers based on stochastic PDE models, it is necessary to identify PDE model parameters based on the surface height data obtained from kinetic Monte-Carlo simulations to compensate for this model error.

3. Feedback control

In this section, we design a linear state feedback controller for the system of Eq. (13) so that the surface roughness defined in Eq. (15) can be controlled to a desired level.

3.1. Model reduction

Owing to its infinite-dimensional nature, the system of Eq. (13) cannot be directly used for the design of controllers that can be implemented in practice (i.e., the practical implementation of controllers which are designed on the basis of this system will require the computation of infinite sums which cannot be done by a computer). Instead, we will base the controller design on finite-dimensional approximations of this system. Subsequently, we will show that the resulting controller will enforce the desired control objectives in the closed-loop infinite-dimensional system.

Specifically, we rewrite the system of Eq. (13) as follows:

$$\begin{aligned} \frac{dx_s}{dt} &= A_s x_s + B_s u + \xi_s \\ \frac{dx_f}{dt} &= A_f x_f + B_f u + \xi_f \end{aligned} \tag{16}$$

where $x_s = [\alpha_1 \dots \alpha_m \beta_1 \dots \beta_m]^T$, $x_f = [\alpha_{m+1} \beta_{m+1} \dots]^T$, $A_s = \text{diag}[\lambda_1 \dots \lambda_m \lambda_1 \dots \lambda_m]$, $A_f = \text{diag}[\lambda_{m+1} \lambda_{m+1} \lambda_{m+2} \lambda_{m+2} \dots]$, $u = [u_1 \dots u_p]$, $\xi_s = [\xi_\alpha^1 \dots \xi_\alpha^m \xi_\beta^1 \dots \xi_\beta^m]$, and $\xi_f = [\xi_\alpha^{m+1} \xi_\beta^{m+1} \dots]$,

$$B_s = \begin{bmatrix} b_{1\alpha_1} & \dots & b_{p\alpha_1} \\ \vdots & \ddots & \vdots \\ b_{1\alpha_m} & \dots & b_{p\alpha_m} \\ b_{1\beta_1} & \dots & b_{p\beta_1} \\ \vdots & \ddots & \vdots \\ b_{1\beta_m} & \dots & b_{p\beta_m} \end{bmatrix};$$

$$B_f = \begin{bmatrix} b_{1\alpha_{m+1}} & \cdots & b_{p\alpha_{m+1}} \\ b_{1\beta_{m+1}} & \cdots & b_{p\beta_{m+1}} \\ b_{1\alpha_{m+2}} & \cdots & b_{p\alpha_{m+2}} \\ b_{1\beta_{m+2}} & \cdots & b_{p\beta_{m+2}} \\ \vdots & \vdots & \vdots \end{bmatrix} \quad (17)$$

We note that in the system of Eq. (16), by selecting m sufficiently large, Λ_f is an unbounded differential operator which is exponentially stable.

Neglecting the x_f subsystem, the following $2m$ -dimensional system is obtained:

$$\frac{d\tilde{x}_s}{dt} = \Lambda_s \tilde{x}_s + B_s u + \xi_s \quad (18)$$

where the tilde symbol in \tilde{x}_s denotes that this state variable is associated with a finite-dimensional system.

3.2. Feedback control design

We design the state feedback controller on the basis of the finite-dimensional system of Eq. (18). To simplify our development, we assume that $p = 2m$ and pick the actuator distribution functions such that B_s^{-1} exists. The state feedback control law then takes the form:

$$u = B_s^{-1}[(\Lambda_{cs} - \Lambda_s)\tilde{x}_s] \quad (19)$$

where the matrix Λ_{cs} contains the desired poles of the closed-loop system; $\Lambda_{cs} = \text{diag}[\lambda_{c\alpha 1} \cdots \lambda_{c\alpha m} \lambda_{c\beta 1} \cdots \lambda_{c\beta m}]$, $\lambda_{c\alpha i}$ and $\lambda_{c\beta i}$ ($1 \leq i \leq m$) are the desired poles of the closed-loop finite-dimensional system, which can be determined from the desired closed-loop surface roughness level.

We first analyze the dependence of the covariances of the states α_n and β_n ($n = 1, \dots, m$) on the poles of the finite-dimensional system of Eq. (18). Then, we will show in Section 3.3 that the surface roughness of the infinite-dimensional system of Eq. (13) can be controlled to the desired level by using the state feedback controller of Eq. (19), which only uses a finite number of actuators.

By applying the controller of Eq. (19) to the system of Eq. (18), the closed-loop system takes the form:

$$\frac{d\tilde{x}_s}{dt} = \Lambda_{cs} \tilde{x}_s + \xi_s(t) \quad (20)$$

If all eigenvalues of Λ_{cs} have negative real part, the covariance matrix of $\tilde{x}_s(t)$, $P(t) = \langle \tilde{x}_s(t)\tilde{x}_s(t)^T \rangle$ converges to $P(\infty)$, which is the unique positive definite solution to the Lyapunov equation (Hotz & Skelton, 1987):

$$\Lambda_{cs} P + P \Lambda_{cs} + R_1 = 0 \quad (21)$$

where $R_1 = \langle \xi_s(t)\xi_s(t)^T \rangle$. Eq. (21) cannot be solved, in general, analytically. However, for the specific system considered in this work, the analytical solution for $P(\infty)$ can be obtained

as follows:

$$P(\infty) = \begin{bmatrix} P_\alpha(\infty) & 0 \\ 0 & P_\beta(\infty) \end{bmatrix} \quad (22)$$

where $P_\alpha(\infty) = \text{diag}\langle \alpha_1(\infty)^2 \rangle \cdots \langle \alpha_m(\infty)^2 \rangle$, $P_\beta(\infty) = \text{diag}\langle \beta_1(\infty)^2 \rangle \cdots \langle \beta_m(\infty)^2 \rangle$. $\langle \alpha_n(\infty)^2 \rangle$ and $\langle \beta_n(\infty)^2 \rangle$ ($n = 1, \dots, m$) can be computed by using the following expressions:

$$\langle \alpha_n(\infty)^2 \rangle = -\frac{\sigma^2}{2\lambda_{c\alpha_n}}; \quad \langle \beta_n(\infty)^2 \rangle = -\frac{\sigma^2}{2\lambda_{c\beta_n}} \quad (23)$$

From Eq. (23), we can see that by assigning the closed-loop poles $\lambda_{c\alpha_n}$ and $\lambda_{c\beta_n}$ ($n = 1, \dots, m$) at desired locations, the covariances of the states α_n and β_n ($n = 1, \dots, m$) can be controlled to desired levels. Therefore, according to Eq. (15), the contribution to the surface roughness from the finite-dimensional system of Eq. (18) can be controlled to the desired level.

3.3. Analysis of the closed-loop infinite-dimensional system

In this subsection, we show that when the state feedback controller of Eq. (19) is used to manipulate the poles of the finite-dimensional system of Eq. (18), the contribution to the surface roughness from the α_f and β_f subsystem of the system of Eq. (16) is bounded and can be made arbitrarily small by increasing the dimension of the x_s subsystem.

By applying the feedback controller of Eq. (19) into the infinite-dimensional system of Eq. (16), we obtain the following closed-loop system:

$$\begin{aligned} \frac{dx_s}{dt} &= \Lambda_{cs} x_s + \xi_s \\ \frac{dx_f}{dt} &= \Lambda_\epsilon x_s + \Lambda_f x_f + \xi_f \end{aligned} \quad (24)$$

where $\Lambda_\epsilon = B_f B_s^{-1}(\Lambda_{cs} - \Lambda_s)$.

The boundedness of the state of the above system follows directly from the stability of the matrices Λ_{cs} and Λ_f and the structure of the system, where the x_s subsystem is independent of the x_f state (see Christofides, 2001; Christofides & Daoutidis, 1997 for results and techniques for analyzing the stability properties of such systems).

Due to the structure of the eigenspectrum of operator A (Section 2.2), the effect of the control action computed from Eq. (19) to the poles of the x_f subsystem can be reduced by increasing m . Therefore, by picking m sufficiently large, the $\Lambda_\epsilon x_s$ can be made very small compared to $\Lambda_f x_f$ and thus, the closed-loop system of Eq. (24) can be adequately described by the following system:

$$\begin{aligned} \frac{dx_s}{dt} &= \Lambda_{cs} x_s + \xi_s \\ \frac{dx_f}{dt} &= \Lambda_f x_f + \xi_f \end{aligned} \quad (25)$$

On the basis of the above system, it can be shown that the covariance of the state of the x_f subsystem converges to $[(\alpha_{m+1}(\infty)^2) \langle \beta_{m+1}(\infty)^2 \rangle \cdots \cdots]$, where

$$\begin{aligned} \langle \alpha_n(\infty)^2 \rangle &= \frac{\sigma^2}{2n^2(\kappa n^2 - \nu)}; \\ \langle \beta_n(\infty)^2 \rangle &= \frac{\sigma^2}{2n^2(\kappa n^2 - \nu)}; \quad n > m \end{aligned} \quad (26)$$

Therefore, for m sufficiently large, the overall contribution to the surface roughness from the x_f subsystem in Eq. (16), $\sqrt{\langle r_f^2 \rangle}$ can be computed as follows:

$$\sqrt{\langle r_f^2 \rangle} = \sqrt{\frac{1}{2\pi} \sum_{n=m+1}^{\infty} \left[\frac{\sigma^2}{n^2(\kappa n^2 - \nu)} \right]} \quad (27)$$

Clearly, as $m \rightarrow \infty$, the contribution to the surface roughness from the x_f subsystem goes to zero.

In summary, under the controller of Eq. (19), the closed-loop surface roughness, for m sufficiently large, can be adequately described by the following expression:

$$\sqrt{\langle r^2 \rangle} = \sigma \sqrt{\frac{1}{2\pi} \left\{ \lambda^* + \sum_{n=m+1}^{\infty} \left[\frac{1}{n^2(\kappa n^2 - \nu)} \right] \right\}} \quad (28)$$

where $\lambda^* = \sum_{i=1}^m (-1/2\lambda_{c\alpha_i} - 1/2\lambda_{c\beta_i})$ and $\lambda_{c\alpha_i}$ and $\lambda_{c\beta_i}$ are closed-loop poles of the finite-dimensional system of Eq. (20).

Remark 3. Note that in order to regulate the surface roughness to a desired level, $\langle \sqrt{r_d^2} \rangle$, the number of actuators should be large enough so that the value of $\langle \sqrt{r_d^2} \rangle$ is achievable. Specifically, the number of actuators, $2m$ should be selected such that the following inequality holds:

$$\sqrt{\langle r_d^2 \rangle} > \sigma \sqrt{\frac{1}{2\pi} \left\{ \sum_{n=m+1}^{\infty} \left[\frac{1}{n^2(\kappa n^2 - \nu)} \right] \right\}} \quad (29)$$

This is because the closed-loop stability requires that $\lambda_{c\alpha_i} < 0$ and $\lambda_{c\beta_i} < 0$ (for $i = 1, \dots, m$), and thus, $\lambda^* > 0$ in Eq. (28).

Remark 4. Note that to control the closed-loop surface roughness to $\sqrt{\langle r_d^2 \rangle}$, we need to design a controller to assign the poles of the finite-dimensional system of Eq. (20) to appropriate values so that the following equation holds:

$$\lambda^* = \frac{2\pi(\langle r_d^2 \rangle - \langle r_f^2 \rangle)}{\sigma^2} \quad (30)$$

The controller which assigns the poles of the system of Eq. (20) to satisfy Eq. (30) is not unique. Consequently, for a fixed number of actuators, p , the controller that can regulate the closed-loop surface roughness to a desired level is also not unique. Furthermore, we note that robust control methods (Christofides, 1998; Christofides & Baker,

1999), which utilize bounds of the noise terms, can be employed to design controllers that can achieve arbitrary degree of attenuation of the effect of noise on the PDE system state.

Remark 5. We note that a full-scale model of a sputtering process would consist of a 2D-lattice representation of the surface. Although we developed the method for feedback control design based on the 1D-lattice representation of the surface, it is possible to apply the proposed method to control the surface roughness of sputtering processes taking place in two-dimensional surfaces. In a two-dimensional process, the feedback control design and the analysis of the closed-loop system will be based on the model of Eq. (16). Moreover, Eq. (16) will be obtained by solving the eigenvalue/eigenfunction problem of the operator A in the two-dimensional spatial domain with appropriate boundary conditions. After Eq. (16) is obtained, the method for control design and closed-loop analysis presented above can be applied to control the surface roughness for two-dimensional surfaces described by stochastic PDEs.

4. Simulation results

In this section, we present applications of the method followed for the design of the state feedback controller to control three different sputtering processes. In all processes, the sputtering occurs on a lattice containing 200 sites. Therefore, $a = 0.0314$. The rate of bombardment for each surface site is $\bar{r}_b = 1s^{-1}$ in the open-loop system. Specifically, the following three processes are studied in this work.

Process 1. Only surface erosion is considered, which is corresponding to $f = 1$ in the sputtering process model in Section 2.1. Plus, we set $Y(\phi) \equiv 1$ and the probability with which a particle is removed from a surface site is $1 - P_e$, where P_e is determined by the box rule shown in Fig. 1.

Process 2. Both erosion and surface diffusion are considered with $\bar{f} = 0.5$. The sputtering yield function, $Y(\phi_i) \equiv 1$. If a randomly selected surface site is subject to erosion, the probability with which a particle is removed from a surface site is P_e , where P_e is determined by the box rule shown in Fig. 1. If a randomly selected surface site is subject to diffusion, the diffusion probability, $w_{i \rightarrow j}$ is computed according to Eq. (3) with $\beta J = 2.0$.

Process 3. Both erosion and surface diffusion are considered with $\bar{f} = 0.5$. The sputtering yield function, $Y(\phi_i)$ is a nonlinear function of ϕ_i , which takes the form of Eq. (1). y_0 , y_1 and y_2 are chosen such that $Y(0) = 0.5$, $Y(\pi/2) = 0$ and $Y(1) = 1$ (Cuerno et al., 1995). If a randomly selected surface site is subject to erosion, the probability with which a particle is removed from a surface site is $Y(\phi_i)P_e$, where P_e is determined by the box rule shown in Fig. 1. If a randomly selected surface site is subject to diffusion, the diffusion probability, $w_{i \rightarrow j}$ is computed according to Eq. (3) with $\beta J = 2.0$.

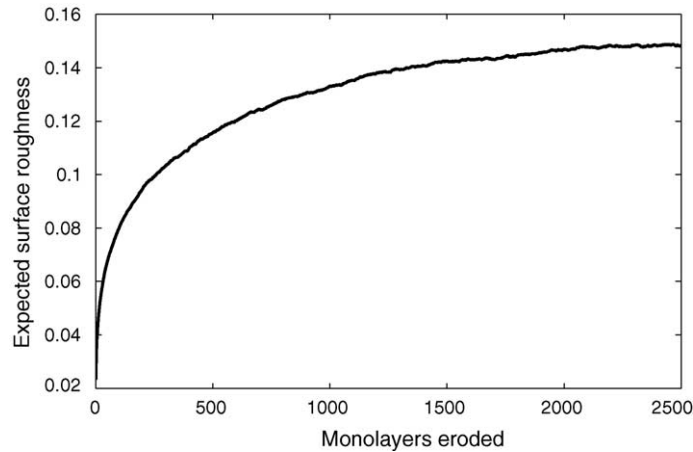


Fig. 2. The open-loop profile of the expected surface roughness in Process 1 computed from the kinetic Monte-Carlo simulations.

4.1. Feedback control of surface roughness in Process 1

According to Cuerno et al. (1995), in the stochastic KSE model of Eq. (5), the nonlinear term corresponds to the effect of the nonlinear function $Y(\phi)$ and κ accounts for the surface diffusion. By setting $Y(\phi) \equiv 1$ and $f = 1$, the surface roughness has the scaling properties of the Edwards–Wilkinson equation (Edwards & Wilkinson, 1982). The open-loop surface roughness converges to a finite value (see Fig. 2). This is because by setting the erosion probability equal to $1 - P_e$, one favors the erosion of peaks as compared to valleys, which is a smoothing mechanism preventing the instability of surface roughness in the sputtering process.

The problem of controlling surface roughness of a deposition process whose surface height fluctuations are described by the Edwards–Wilkinson equation has been solved in Lou and Christofides (2004b). In this case study, we design a feedback controller based on the stochastic PDE model, which takes the form of the Edwards–Wilkinson equation, of the sputtering process. The model parameters are identified by using data of the evolution of surface height obtained from kinetic Monte-Carlo simulations so that the prediction of the surface roughness from the solution of the stochastic PDE model of the process is consistent to that from the kinetic Monte-Carlo simulations. Then, we apply the designed controller to the kinetic Monte-Carlo model of the sputtering process to control the surface roughness of this process to a desired level.

4.1.1. Model identification

Since the surface roughness in this sputtering process has the same scaling properties to that of the Edwards–Wilkinson equation (Edwards & Wilkinson, 1982), the following stochastic PDE model is used to describe height fluctuation of the surface in Process 1:

$$\frac{\partial h}{\partial t} = -\nu \frac{\partial^2 h}{\partial x^2} + \xi(x, t) \quad (31)$$

$$\langle \xi(x, t) \xi(x', t') \rangle = \sigma^2 \delta(x - x') \delta(t - t')$$

where $\nu < 0$. By expanding h in an infinite series in terms of $\phi(x)$ and $\psi(x)$ as in Eq. (12), the following system of infinite stochastic ODEs is obtained:

$$\begin{aligned} \frac{d\alpha_n}{dt} &= \nu n^2 \alpha_n + \xi_\alpha^n(t) \\ \frac{d\beta_n}{dt} &= \nu n^2 \beta_n + \xi_\beta^n(t); \quad n = 1, \dots, \infty \end{aligned} \quad (32)$$

Based on Eq. (32), we can obtain the following expressions for $\alpha_n(t)$ and $\beta_n(t)$:

$$\begin{aligned} \alpha_n(t) &= \alpha_n(0)e^{\nu n^2 t} + \int_0^t e^{\nu n^2(t-\tau)} \xi_\alpha^n(\tau) d\tau \\ \beta_n(t) &= \beta_n(0)e^{\nu n^2 t} + \int_0^t e^{\nu n^2(t-\tau)} \xi_\beta^n(\tau) d\tau; \quad n = 1, \dots, \infty \end{aligned} \quad (33)$$

If the initial surface is flat, e.g., $\alpha_n(0) = 0$ and $\beta_n(0) = 0$, for $n = 1, \dots, \infty$, the covariance of $\alpha_n(t)$ and $\beta_n(t)$ can be computed as follows by using Result 1:

$$\langle \alpha_n(t)^2 \rangle = \langle \beta_n(t)^2 \rangle = \sigma^2 \left(\frac{e^{2\nu n^2 t} - 1}{2\nu n^2} \right); \quad n = 1, \dots, \infty \quad (34)$$

Based on Eq. (34), the values of ν and σ can be identified by using the data of $\langle \alpha_n(t)^2 \rangle$ or $\langle \beta_n(t)^2 \rangle$, which can be obtained from kinetic Monte-Carlo simulations of the same sputtering process. The kinetic Monte-Carlo simulation algorithm used to simulate the sputtering process is described as follows. In this algorithm, a trial to execute an event may or may not be successful (Ziff, Gulari, & Barshad, 1986). Upon successful realization of an event, the time is advanced by an increment, δt (Fichthorn & Weinberg, 1991).

Monte-Carlo algorithm for Process 1:

- A random number, ζ_1 is first generated to pick a site, i , among all the sites on the 1D-lattice.

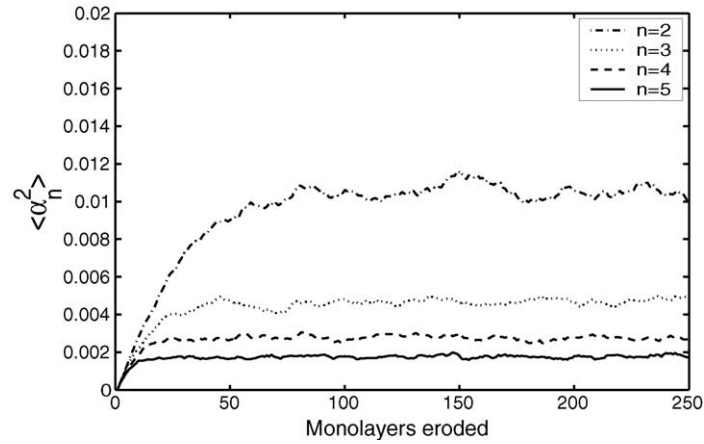


Fig. 3. Evolution of $\langle \alpha_2^2 \rangle$, $\langle \alpha_3^2 \rangle$, $\langle \alpha_4^2 \rangle$ and $\langle \alpha_5^2 \rangle$ in Process 1.

- P_e is computed by using the box rule shown in Fig. 1 and the center of the box is the surface particle on site i .
- The second random number, ζ_2 in the $(0, 1)$ interval is generated.
- If $\zeta_2 > 1 - P_e$, no Monte-Carlo event is executed and the trial is not successful.
- If $\zeta_2 < 1 - P_e$ the surface particle on site i is removed and a time increment, δt is computed by using the following expression:

$$\delta t = -\frac{\ln \zeta_3}{\sum_{i=1}^N (1 - P_{e_i})} \quad (35)$$

where ζ_3 is a random number in the $(0, 1)$ interval and P_{e_i} is computed by using the box rule shown in Fig. 1 in which the center of the box is the surface particle at site i .

- Upon the successful realization of one Monte-Carlo event (a surface particle is removed from site i), α_n or β_n can be updated by using the following expression:

$$\begin{aligned} \alpha_n^{\text{new}} &= \alpha_n^{\text{old}} + \frac{a[\psi(n, z_i - a/2) - \psi(n, z_i + a/2)]}{n} \\ \beta_n^{\text{new}} &= \beta_n^{\text{old}} + \frac{a[\phi(n, z_i + a/2) - \phi(n, z_i - a/2)]}{n} \end{aligned} \quad (36)$$

where a is the lattice parameter and z_i is the coordinate of the center of site i .

Fig. 2 shows the open-loop profile of the expected surface roughness in Process 1 from kinetic Monte-Carlo simulations. The expected surface roughness is obtained by averaging surface roughness profiles from 1000 independent simulation runs by using the same simulation parameters. The expected surface roughness converges to about 0.15 after about 2500 monolayers are eroded.

Fig. 3 shows the open-loop profiles of $\langle \alpha_n^2 \rangle$ for $n = 2, 3, 4$, and 5. Each profile is obtained by averaging the profiles of α_n^2 from 1000 independent kinetic Monte-Carlo simulation runs using the same simulation parameters.

Using the profiles shown in Fig. 3, we identify the values of ν and σ of Eq. (31) based on Eq. (34). While $\nu < 0$, as

$t \rightarrow \infty$, $1/\langle \alpha_n(\infty)^2 \rangle = -2\nu n^2/\sigma^2$. $1/\langle \alpha_n(\infty)^2 \rangle$ versus n for $n = 2, 3, 4$, and 5 is marked in Fig. 4 by open circle. Using the method of least-mean-square, we fit the data marked in Fig. 4 using a parabolic equation, $y = 23.07n^2$, which is plotted in Fig. 4 by using the dotted line. Therefore, we obtain the following relationship between ν and σ :

$$-\frac{2\nu}{\sigma^2} = 23.07 \quad (37)$$

Furthermore, based on Eq. (34), we can get the following equation for ν :

$$-\frac{\ln[(2\nu n^2/\sigma^2)\langle \alpha_n(t)^2 \rangle + 1]}{n^2} = -2\nu t \quad (38)$$

Therefore, if we plot $-\ln[2\nu n^2/\sigma^2\langle \alpha_n(t)^2 \rangle + 1]/n^2$ versus t , the slope is -2ν . This plot is shown in Fig. 5. In Fig. 5, four lines are plotted for $n = 2, 3, 4$, and 5. It is clear that these four lines have almost identical slopes, which means that the

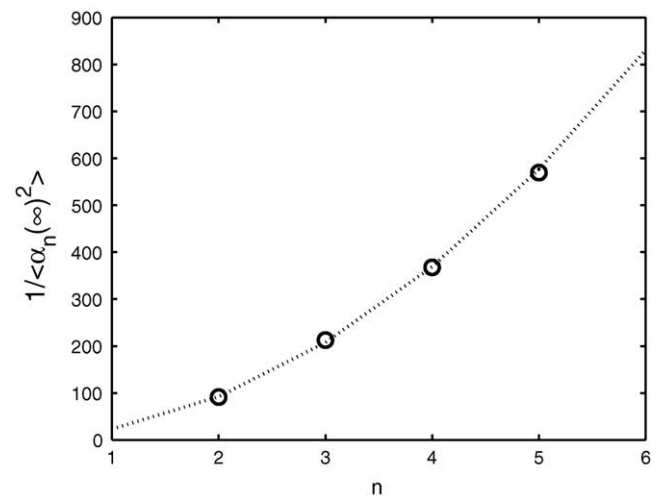


Fig. 4. $1/\langle \alpha_n(\infty)^2 \rangle$ vs. n for $n = 2, 3, 4$, and 5 (marked by open circle) and the curve of $y = 23.07n^2$ (dotted line) in Process 1.

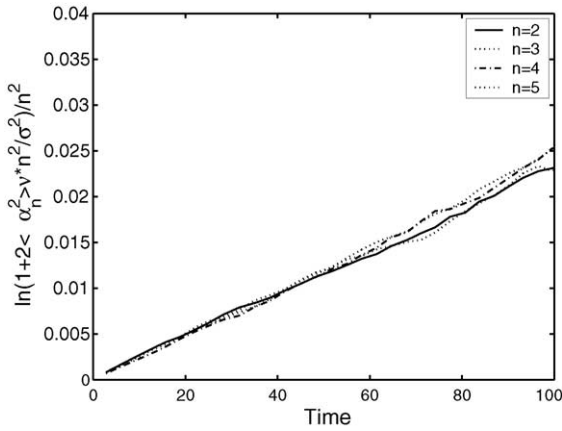


Fig. 5. $-\ln[2\nu n^2/\sigma^2(\alpha_n(t)^2) + 1]/n^2$ vs. t for $n = 2, 3, 4,$ and 5 in Process 1.

value of ν identified in this way is independent of the data set used in the identification.

From Fig. 5, the value of ν is identified as $\nu = -1.2 \times 10^{-4}$. Then, by using Eq. (37), $\sigma = 3.2 \times 10^{-3}$. Using the identified parameters of Eq. (31), we compute the expected surface roughness in Process 1 based on Eq. (31). An 80th order stochastic ordinary differential equation approximation of the system of Eq. (31) is used to simulate the process (the use of higher-order approximations led to identical numerical results, thereby implying that the following simulation runs are independent of the discretization). The δ function involved in the covariances of ξ_α^n and ξ_β^n is approximated by $1/\Delta t$, where Δt is the integration time step. There is a small difference between the expected surface roughness profile obtained from kinetic Monte-Carlo simulations and that from the solution of the Edwards–Wilkinson equation with $\nu = -1.2 \times 10^{-4}$ and $\sigma = 3.2 \times 10^{-3}$ and this difference can be compensated by increasing the value of σ from 3.2×10^{-3} to 3.4×10^{-3} . In Fig. 6, we compare the expected value of the open-loop surface roughness of Process 1 from the solution of the Edwards–Wilkinson equation of Eq. (31) with $\nu = -1.2 \times 10^{-4}$ and $\sigma = 3.4 \times 10^{-3}$ to that from kinetic Monte-Carlo simulations. The two profiles are almost identical. Therefore, by using the stochastic PDE model of Eq. (31) with the identified model parameters, we can predict the evolution of the expected surface roughness in this sputtering process. The stochastic PDE model of Eq. (31) is used as the basis for controller design.

4.1.2. Feedback control design

Our control objective is to control the expected surface roughness in Process 1 to a desired value. We design a state feedback controller based on a 20th order stochastic ODE approximation constructed by using the first 20 eigenmodes of the system of Eq. (13) with identified model parameters $\nu = -1.2 \times 10^{-4}$, $\sigma = 3.4 \times 10^{-3}$ and $\kappa = 0$. Twenty control actuators are used to control the system. The i th actuator

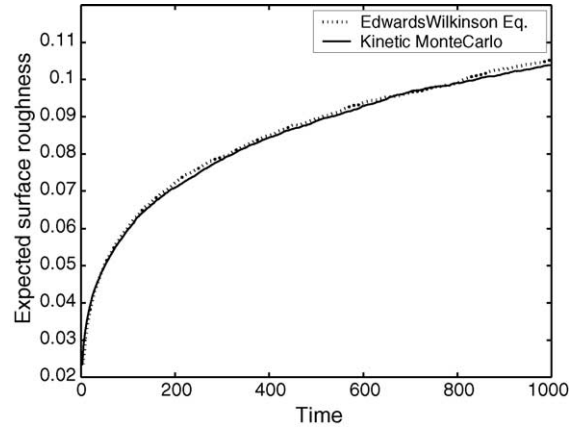


Fig. 6. Comparison of the open-loop profile of the expected surface roughness from the kinetic Monte-Carlo simulator (solid line) and that from the solution of the Edwards–Wilkinson equation with $\nu = -1.2 \times 10^{-4}$ and $\sigma = 3.4 \times 10^{-3}$ (dotted line) in Process 1.

distribution function is taken to be:

$$b_i(z) = \begin{cases} \frac{1}{\sqrt{\pi}} \sin(iz); & i = 1, \dots, 10 \\ \frac{1}{\sqrt{\pi}} \cos[(i - 10)z]; & i = 11, \dots, 20 \end{cases} \quad (39)$$

The desired closed-loop surface roughness is 0.053 in this simulation. Using Eq. (28), we design the state feedback controller such that $\lambda_{c\alpha_i} = \lambda_{c\beta_i} = -0.027$, for $i = 1, \dots, 10$. Then, we apply the designed controller to the kinetic Monte-Carlo model of Process 1 to control the surface roughness to the desired level. In this simulation, the controller is implemented by manipulating the bombardment rate of particles across the surface. Specifically, the bombardment rate on site i at time t is determined according to the following expression:

$$r_b(i, t) = \bar{r}_b + \frac{(\sum_{j=1}^{20} b_j(z_i)u_j(t))}{a} \quad (40)$$

The following simulation algorithm is used to run the kinetic Monte-Carlo simulations for the closed-loop system. First, a random number is generated to pick a site among all the sites on the 1D-lattice; the probability that a surface site is picked is proportional to the bombardment rate on this site, which is computed by using Eq. (40). Then, P_e is computed by using the box rule shown in Fig. 1 and the center of the box is the surface particle on site i . The second random number, ζ_2 in the $(0, 1)$ interval is generated. If $\zeta_2 > 1 - P_e$ no Monte-Carlo event is executed. If $\zeta_2 < 1 - P_e$ the surface particle on site i is removed. Once a particle is removed, the first 20 states ($\alpha_1, \dots, \alpha_{10}$ and $\beta_1, \dots, \beta_{10}$) are updated and new control actions are computed to update the spatially distributed bombardment rate across the surface.

The closed-loop system simulation results are shown in Fig. 7. The dashed line shows the expected surface roughness, which is the average of surface roughness profiles obtained from 200 independent runs, under feedback control.

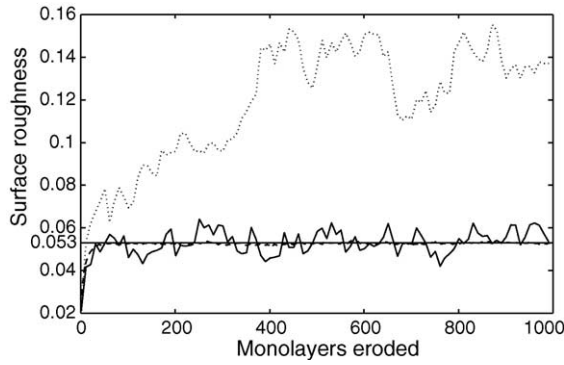


Fig. 7. Closed-loop surface roughness profiles in Process 1. (a) The closed-loop surface roughness profile from one simulation run (solid line); (b) the expected closed-loop surface roughness profile obtained from 200 independent simulation runs (dashed line); and (c) the open-loop surface roughness profile from one simulation run (dotted line).

We can see that the controller successfully drives the expected surface roughness to the desired level. The solid line shows the surface roughness profile under feedback control from one simulation run; due to the stochastic nature of the deposition process, stochastic fluctuations can be observed in the closed-loop surface roughness profile, but the surface roughness is very close to the set-point value under feedback control. For the sake of comparison, the dotted line shows a surface roughness profile from one open-loop simulation run. We can see that under feedback control, a much lower surface roughness can be achieved.

Remark 6. Note that the number of control actuators needed to regulate the expected closed-loop surface roughness to a desired level, $\sqrt{r_d^2}$, depends on the value of $\sqrt{r_d^2}$. In this simulation study, twenty control actuators are used to regulate the expected closed-loop surface roughness to 0.053. However, this is not the minimum number of control actuators required to achieve a closed-loop surface roughness of 0.053. For a fixed number of control actuators available, the lowest achievable closed-loop surface roughness can be computed by using Eq. (29) and some results are listed in Table 1. A minimum of two control actuators are required if the desired surface roughness is 0.099 and a minimum of ten control actuators are required if the desired surface roughness is 0.053.

4.2. Feedback control of surface roughness in Process 2

Compare to Process 1, surface diffusion is added in Process 2. In this case study, $\bar{f} = 0.5$ and $J/k_B T = 2.0$. The presence of two mechanisms results to more complicated process dynamics and the open-loop surface roughness is unstable, e.g., the surface roughness goes to infinity as $t \rightarrow \infty$. In

Table 1

Number of control actuators vs. the lowest achievable closed-loop surface roughness

Number of control actuators	Lowest achievable closed-loop surface roughness
2	0.099
4	0.078
6	0.066
8	0.058
10	0.053
20	0.038
30	0.031
40	0.027

this case study, our control objective is to stabilize the closed-loop surface roughness to a finite value. We first study the dynamics of the surface roughness in this sputtering process and identify the number of unstable modes in this process. It turns out that the number of unstable modes is finite. Then, we design a model-based state feedback controller, which employs more control actuators than the number of unstable modes, to stabilize the surface roughness to a finite value.

4.2.1. Open-loop dynamics

We run kinetic Monte-Carlo simulations to study the dynamics of the open-loop surface roughness and the evolution of covariance of α_n and β_n in this sputtering process. The kinetic Monte-Carlo simulation algorithm and the method to compute $\alpha_n(t)$ or $\beta_n(t)$ are as follows:

- The first random number, ζ_1 is generated to pick a site, i , among all the sites on the 1D-lattice.
- The second random number, ζ_2 in the $(0, 1)$ interval, is generated to decide whether the chosen site is subject to erosion ($\zeta_2 < \bar{f}$) or diffusion ($\zeta_2 > \bar{f}$).
- If the chosen site is subject to erosion, P_e is computed by using the box rule shown in Fig. 1 and the center of the box is the surface particle on site i . Then, another random number ζ_{e3} in the $(0, 1)$ interval is generated. If $\zeta_{e3} < P_e$ the surface particle on site i is removed. Otherwise, no Monte-Carlo event is executed.
- If the chosen site is subject to diffusion, a side neighbor, j ($j = i + 1$ or $i - 1$ in the case of 1D-lattice) is randomly picked and the hopping rate, $w_{i \rightarrow j}$, is computed by using Eq. (3). Then, another random number ζ_{d3} in the $(0, 1)$ interval is generated. If $\zeta_{d3} < w_{i \rightarrow j}$, the surface atom is moved to the new site. Otherwise no Monte-Carlo event is executed.
- Upon the execution of one Monte-Carlo event, α_n or β_n are updated. If the executed event is erosion, α_n or β_n can be updated by using Eq. (36). If the executed event is diffusion from site i to site j , α_n or β_n are updated by using the following expression:

$$\begin{aligned} \alpha_n^{\text{new}} &= \alpha_n^{\text{old}} + \frac{a\{[\psi(n, z_i - a/2) - \psi(n, z_i + a/2)] - [\psi(n, z_j - a/2) - \psi(n, z_j + a/2)]\}}{n} \\ \beta_n^{\text{new}} &= \beta_n^{\text{old}} + \frac{a\{[\phi(n, z_i + a/2) - \phi(n, z_i - a/2)] - [\phi(n, z_j + a/2) - \phi(n, z_j - a/2)]\}}{n} \end{aligned} \quad (41)$$

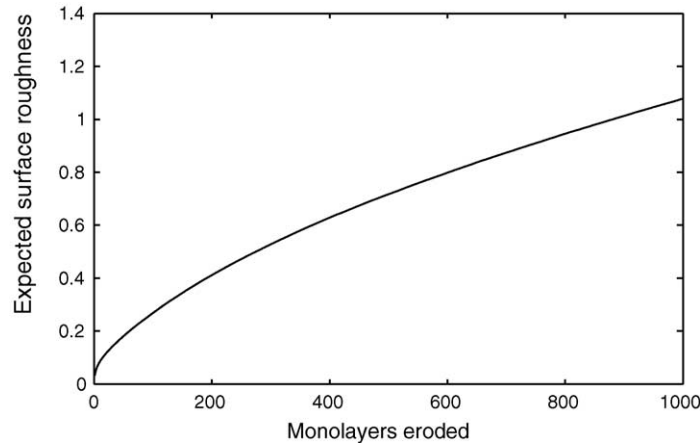


Fig. 8. The open-loop profile of the expected surface roughness in Process 2 from the kinetic Monte-Carlo simulator.

where a is the lattice parameter, z_i is the coordinate of the center of site i and z_j is the coordinate of the center of site j .

Fig. 8 shows the open-loop profile of the expected surface roughness of Process 2 from kinetic Monte-Carlo simulations. The expected surface roughness is obtained by averaging surface roughness profiles from 1000 independent simulation runs by using the same simulation parameters. It is clear that the open-loop expected surface roughness in this sputtering process does not converge to a finite value. Our control objective is to stabilize the closed-loop surface roughness to a finite value. To do this, we identify the number of unstable modes in this process and use more control actuators than the number of unstable modes to stabilize the surface roughness in the closed-loop system.

Fig. 9 shows the open-loop profiles of $\langle \alpha_n^2 \rangle$ for $n = 1, 5, 15,$ and 20 . Each profile is obtained by averaging the profile α_n^2 from 1000 independent simulation runs by using the same simulation parameters.

4.2.2. Feedback control design

In Fig. 9, it is clear that at least the first 15 modes are unstable. Although α_{20}^2 is stable, its magnitude is in the same

order of that of α_1^2 or α_5^2 , which is still significant. The same dynamics are also observed in the open-loop profiles of $\langle \beta_n^2 \rangle$. To this end, we design a state feedback controller based on the first 50 modes of the process (25 modes for the α_n subsystem and 25 modes for the β_n subsystem), which is sufficiently larger than the number of unstable modes (which is about 30) in the process, to stabilize the closed-loop surface roughness to a finite value. Fifty control actuators are used to control the system. The i th actuator distribution function is taken to be:

$$b_i(z) = \begin{cases} \frac{1}{\sqrt{\pi}} \sin(iz); & i = 1, \dots, 25 \\ \frac{1}{\sqrt{\pi}} \cos[(i - 25)z]; & i = 26, \dots, 50 \end{cases} \quad (42)$$

We design the following state feedback controller to control the process:

$$u = B_s^{-1} \Lambda \tilde{x}_s \quad (43)$$

where $\tilde{x}_s = [\alpha_1, \dots, \alpha_{25}, \beta_1, \dots, \beta_{25}]^T$, $\Lambda = -0.01 \times I_{50 \times 50}$ and I is an identity matrix.

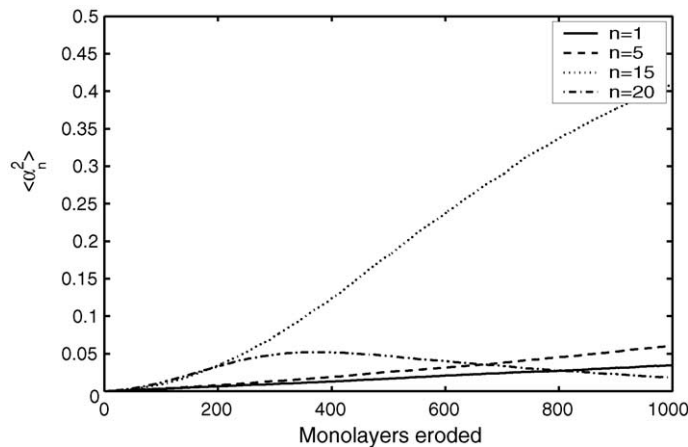


Fig. 9. Evolution of $\langle \alpha_1^2 \rangle$, $\langle \alpha_5^2 \rangle$, $\langle \alpha_{15}^2 \rangle$ and $\langle \alpha_{20}^2 \rangle$ in Process 2.

Then, we apply the designed controller to the kinetic Monte-Carlo model of Process 2 to control the surface roughness to the desired level. In this simulation, the controller is implemented by manipulating the probability that a randomly selected site is subject to erosion rule, f . Specifically, f at site i is determined according to the following expression:

$$f(i) = \frac{\bar{f} + \left(\sum_{j=1}^{50} b_j(z_i) u_j(t) \right) / a}{1 + \left(\sum_{j=1}^{50} b_j(z_i) u_j(t) \right) / a} \quad (44)$$

The following simulation algorithm is used to run the kinetic Monte-Carlo simulations for the closed-loop system. First, a random number, ζ_1 is generated to pick a site, i among all the sites on the 1D-lattice; the probability that a surface site is subject to erosion rules, $f(i)$ is determined by using Eq. (44). Then, the second random number, ζ_2 in the $(0, 1)$ interval is generated. If $\zeta_2 < f(i)$, the site i is subject to erosion, otherwise, the site is subject to diffusion.

If the site i is subject to erosion, P_e is computed by using the box rule shown in Fig. 1 and the center of the box is the surface particle on site i . Another random number, ζ_{e3} in the $(0, 1)$ interval is generated. If $\zeta_{e3} > 1 - P_e$, no Monte-Carlo event is executed and go back to the first step of this algorithm. If $\zeta_{e3} < 1 - P_e$, the surface particle on site i is removed. Otherwise, no Monte-Carlo event is executed.

If the site i is subject to diffusion, a side-neighbor, $j = i + 1$ or $j - 1$ is randomly picked and the probability of a hopping from site i to site j , $w_{i \rightarrow j}$ is computed based on Eq. (3). Then, another random number ζ_{d3} in the $(0, 1)$ interval is generated. If $\zeta_{d3} < w_{i \rightarrow j}$, the surface particle on site i is moved to site j . Otherwise, no Monte-Carlo event is executed.

Once a Monte-Carlo event is executed, the first 50 states ($\alpha_1, \dots, \alpha_{25}$ and $\beta_1, \dots, \beta_{25}$) are updated and new control actions are computed to update the spatially distributed bombardment rate across the surface.

The closed-loop system simulation results are shown in Fig. 10. The dotted line shows the expected surface roughness, which is the average of surface roughness profiles obtained from 200 independent runs, under feedback control.

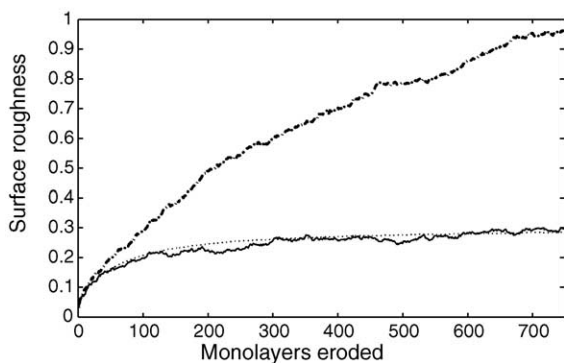


Fig. 10. Closed-loop surface roughness profiles in Process 2. (a) The closed-loop surface roughness profile from one simulation run (solid line); (b) the expected closed-loop surface roughness profile (dotted line); and (c) the open-loop surface roughness profile from one simulation run (dashed line).

We can see that the controller successfully drives the expected surface roughness to a finite value. The solid line shows the surface roughness profile under feedback control from one simulation run; due to the stochastic nature of the deposition process, stochastic fluctuations can be observed in the closed-loop surface roughness profile, but the surface roughness is very close to the expected surface roughness under feedback control. For the sake of comparison, the dashed-line shows a surface roughness profile from one open-loop simulation run. We can see that under feedback control, the surface roughness can be stabilized to a finite value.

4.3. Feedback control of surface roughness in Process 3

In this case study, our control objective is to control the surface roughness in Process 3 to a desired level. In Process 3, both erosion and diffusion are included and the sputtering yield function, $Y(\phi_i)$, is a nonlinear function of ϕ_i as shown in Eq. (1) with $\gamma_0 = 0.5$, $\gamma_1 = 1.0065$ and $\gamma_2 = -0.5065$. The evolution of surface height in this sputtering process is described by the stochastic Kuramoto–Sivashinsky equation of Eq. (5) (Cuerno et al., 1995; Lauritsen et al., 1996). In this case study, we design a feedback controller based on the linearization of the stochastic KSE with appropriately identified parameters. Then, we apply the designed controller to the kinetic Monte-Carlo model of this sputtering process to control the surface roughness of this process to a desired level.

4.3.1. Model identification

The following linearized stochastic Kuramoto–Sivashinsky equation is used as the basis for controller design:

$$\frac{\partial h}{\partial t} = -v \frac{\partial^2 h}{\partial x^2} - \kappa \frac{\partial^4 h}{\partial x^4} + \xi(x, t) \quad (45)$$

where

$$\langle \xi(x, t) \xi(x', t') \rangle = \sigma^2 \delta(x - x') \delta(t - t') \quad (46)$$

By expanding h in an infinite series in terms of $\phi(x)$ and $\psi(x)$ as shown in Eq. (12), the following system of infinite stochastic ODEs is obtained:

$$\begin{aligned} \frac{d\alpha_n}{dt} &= (vn^2 - \kappa n^4) \alpha_n + \xi_\alpha^n(t) \\ \frac{d\beta_n}{dt} &= (vn^2 - \kappa n^4) \beta_n + \xi_\beta^n(t); \quad n = 1, \dots, \infty \end{aligned} \quad (47)$$

Therefore,

$$\begin{aligned} \alpha_n(t) &= \alpha_n(0) e^{(vn^2 - \kappa n^4)t} \\ &\quad + \int_0^t e^{(vn^2 - \kappa n^4)(t-\tau)} \xi_\alpha^n(\tau) d\tau \\ \beta_n(t) &= \beta_n(0) e^{(vn^2 - \kappa n^4)t} \\ &\quad + \int_0^t e^{(vn^2 - \kappa n^4)(t-\tau)} \xi_\beta^n(\tau) d\tau; \quad n = 1, \dots, \infty \end{aligned} \quad (48)$$

If the initial surface is a perfect one, $\alpha_n(0) = 0$ and $\beta_n(0) = 0$. Using Result 1, the covariance of $\alpha_n(t)$ and $\beta_n(t)$ can be computed as follows:

$$\langle \alpha_n(t)^2 \rangle = \langle \beta_n(t)^2 \rangle = \sigma^2 \left[\frac{e^{2(\nu n^2 - \kappa n^4)t} - 1}{2(\nu n^2 - \kappa n^4)} \right]; \quad n = 1, \dots, \infty \quad (49)$$

$$\begin{aligned} \alpha_n^{\text{new}} &= \alpha_n^{\text{old}} + \frac{a\{\psi(n, z_i - a/2) - \psi(n, z_i + a/2)\} - [\psi(n, z_j - a/2) - \psi(n, z_j + a/2)]}{n} \\ \beta_n^{\text{new}} &= \beta_n^{\text{old}} + \frac{a\{\phi(n, z_i + a/2) - \phi(n, z_i - a/2)\} - [\phi(n, z_j + a/2) - \phi(n, z_j - a/2)]}{n} \end{aligned} \quad (50)$$

Based on Eq. (49), the value of ν , κ and σ can be identified from the data of $\langle \alpha_n(t)^2 \rangle$ or $\langle \beta_n(t)^2 \rangle$, which can be obtained from kinetic Monte-Carlo simulation of the same sputtering process. The kinetic Monte-Carlo simulation algorithm and the method to compute $\alpha_n(t)$ or $\beta_n(t)$ are as follows:

- The first random number, ζ_1 is generated to pick a site, i , among all the sites on the 1D-lattice.
- The second random number, ζ_2 in the $(0, 1)$ interval, is generated to decide whether the chosen site, i , is subject to erosion ($\zeta_2 < \bar{f}$) or diffusion ($\zeta_2 > \bar{f}$).
- If the chosen site is subject to erosion, P_e and $Y(\phi_i)$ are computed. P_e is computed by using the box rule shown in Fig. 1 and the center of the box is the surface particle on site i and $Y(\phi_i)$ is computed by using Eq. (1). Then, another random number ζ_{e3} in the $(0, 1)$ interval is generated. If $\zeta_{e3} < P_e Y(\phi_i)$ the surface particle on site i is removed. Otherwise, no Monte-Carlo event is executed.
- If the chosen site is subject to diffusion, a side neighbor, j ($j = i + 1$ or $i - 1$ in the case of 1D-lattice) is randomly picked and the hopping rate, $w_{i \rightarrow j}$, is computed by using Eq. (3). Then, another random number ζ_{d3} in the $(0, 1)$

interval is generated. If $\zeta_{d3} < w_{i \rightarrow j}$, the surface atom is moved to the new site. Otherwise no Monte-Carlo event is executed.

- Upon the execution of one Monte-Carlo event, α_n or β_n are updated. If the executed event is erosion, α_n or β_n can be updated by using Eq. (36). If the executed event is diffusion from site i to site j , α_n or β_n are updated by using the following expression:

where a is the lattice parameter and z_i is the coordinate of the center of site i .

Fig. 11 shows the open-loop profile of the expected surface roughness of Process 3 from kinetic Monte-Carlo simulations. The expected surface roughness is obtained by averaging surface roughness profiles from 1000 independent simulation runs by using the same simulation parameters. Our control objective is to control the surface roughness in this sputtering process to a desired level. To achieve this objective, we identify the parameters of the model of Eq. (47) so that the surface roughness predicted by Eq. (47) is consistent to that obtained from kinetic Monte-Carlo simulations of the same sputtering process. Then, we design a feedback controller based on the process model of Eq. (47) with the identified parameters to control the surface roughness in this process.

Fig. 12 shows the open-loop profiles of $\langle \alpha_n^2 \rangle$ for $n = 20, 22, 25$, and 30 . Each profile is obtained by averaging the profile α_n^2 from 1000 independent simulation runs by using the same simulation parameters.

Using the profiles shown in Fig. 12, we identify the values of ν , κ and σ of Eq. (47) based on Eq. (49). When $\nu > 0$, $\kappa > 0$ and n is sufficient large, $\nu n^2 - \kappa n^4 < 0$. Therefore, as $t \rightarrow \infty$, $1/\langle \alpha_n(\infty)^2 \rangle = 2(\kappa n^4 - \nu n^2)/\sigma^2$. $1/\langle \alpha_n(\infty)^2 \rangle$ versus n for $n = 20, 21, \dots, 30$ is marked in Fig. 13 by open

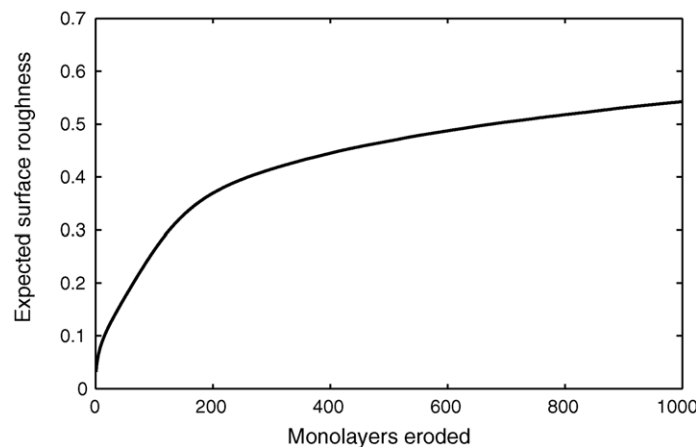


Fig. 11. The open-loop profile of the expected surface roughness in Process 3 from the kinetic Monte-Carlo simulator.

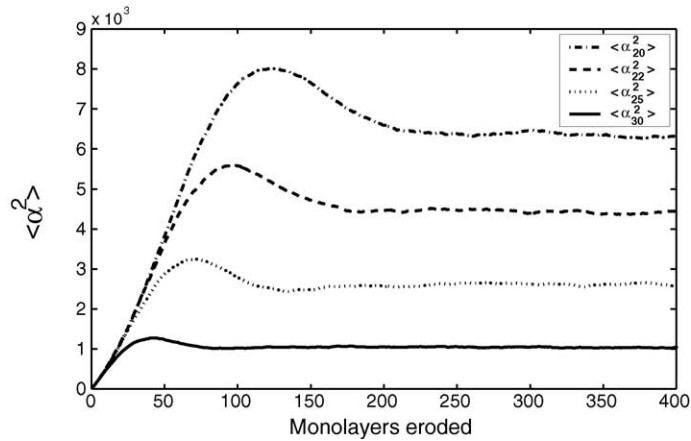


Fig. 12. Evolution of $\langle \alpha_{20}^2 \rangle$, $\langle \alpha_{22}^2 \rangle$, $\langle \alpha_{25}^2 \rangle$ and $\langle \alpha_{30}^2 \rangle$ in Process 3.

circle. Using the method of least-mean-square, we fit the data marked in Fig. 13 using a fourth order polynomial, $y = 1.45 \times 10^{-3}n^4 - 0.26n^2$, which is plotted in Fig. 13 using the dotted line. Therefore, we obtain the following relationships between ν , σ and κ , σ :

$$\frac{2\nu}{\sigma^2} = 0.26; \quad \frac{2\kappa}{\sigma^2} = 1.45 \times 10^{-3} \quad (51)$$

Furthermore, based on Eq. (49), we can get the following equations for ν and κ :

$$\frac{\ln[2(\nu n^2 - \kappa n^4)/\sigma^2 \langle \alpha_n(t)^2 \rangle + 1]}{2n^2} = (\nu - \kappa n^2)t \quad (52)$$

Therefore, if we plot $\ln[2(\nu n^2 - \kappa n^4)/\sigma^2 \langle \alpha_n(t)^2 \rangle + 1]/2n^2$ versus t , the slope is $\nu - \kappa n^2$. This plot is shown in Fig. 14. In Fig. 14, seven lines are plotted for $n = 20, 22, 24, 26, 28,$ and 30 . It is clear that there is an almost linear relationship between $\ln[2(\nu n^2 - \kappa n^4)/\sigma^2 \langle \alpha_n(t)^2 \rangle + 1]/2n^2$ and t .

To identify the values of ν and κ , the slopes of the lines in Fig. 14 versus n are marked in Fig. 15 by open circle. Using the method of least-mean-square, we fit the data marked in

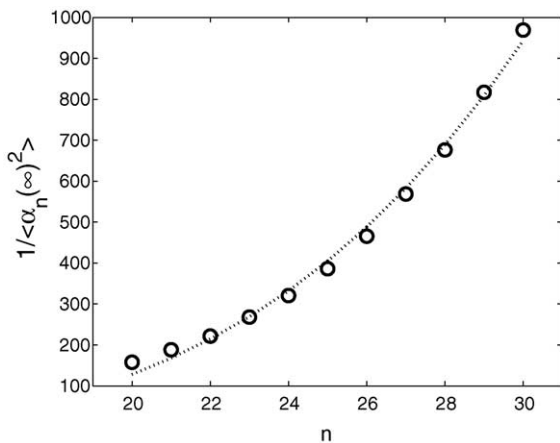


Fig. 13. $1/\langle \alpha_n(\infty)^2 \rangle$ vs. n for $n = 20, 21, \dots, 30$ (marked by open circle) and the curve of $y = 1.45 \times 10^{-3}n^4 - 0.26n^2$ (dotted line) in Process 3.

Fig. 15 using a second order polynomial, $y = 3.27 \times 10^{-6} - 1.34 \times 10^{-8}n^2$, which is plotted in Fig. 15 using the dotted line. Therefore, the values of ν and κ are identified as follows:

$$\nu = 3.27 \times 10^{-6}; \quad \kappa = 1.34 \times 10^{-8} \quad (53)$$

The value of σ is determined by using Eq. (51) and Eq. (53). If we compute the value of σ using $\nu = 3.27 \times 10^{-6}$ and $2\nu/\sigma^2 = 0.26$, we can obtain $\sigma_\nu = 5.0 \times 10^{-3}$. However, if we compute the value of σ using $\kappa = 1.34 \times 10^{-8}$ and $2\kappa/\sigma^2 = 1.45 \times 10^{-3}$, we can obtain $\sigma_\kappa = 4.29 \times 10^{-3}$. We decide that the value of σ is the average of the value of σ_ν and σ_κ as follows:

$$\sigma = \frac{\sigma_\nu + \sigma_\kappa}{2} = 4.65 \times 10^{-3} \quad (54)$$

Using the identified parameters of Eqs. (53) and (54), we compute the expected surface roughness in Process 3 based on Eq. (45). An 80th order stochastic ordinary differential equation approximation of the system of Eq. (45) is used to simulate the process (the use of higher-order approximations led to identical numerical results, thereby implying that

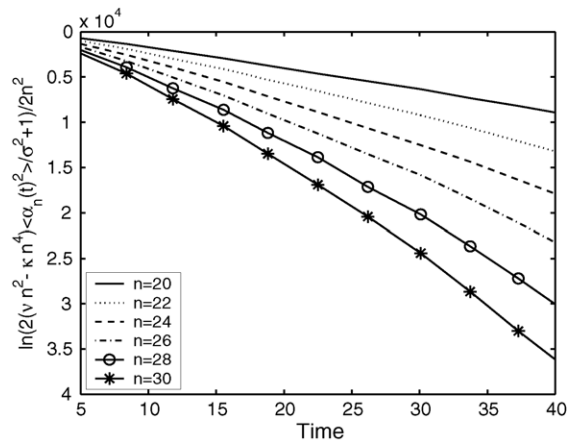


Fig. 14. $\ln[2(\nu n^2 - \kappa n^4)/\sigma^2 \langle \alpha_n(t)^2 \rangle + 1]/2n^2$ vs. t for $n = 20, 22, 24, 26, 28,$ and 30 in Process 3.

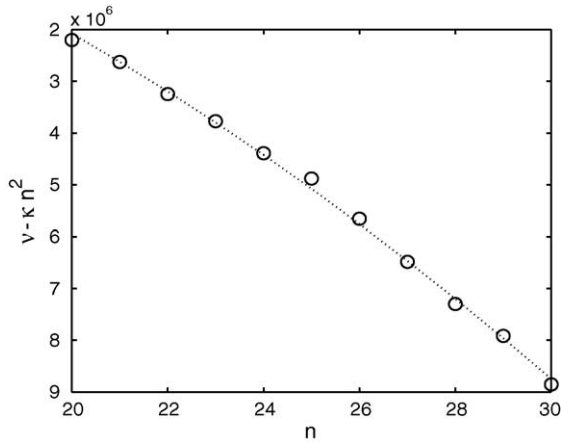


Fig. 15. The slopes of lines in Fig. 14 vs. n for $n = 20, \dots, 30$ (marked by open circle) and the curve of $y = 3.27 \times 10^{-6} - 1.34 \times 10^{-8}n^2$ (dotted line) in Process 3.

the following simulation runs are independent of the discretization). The δ function involved in the covariances of ξ_α^n and ξ_β^n is approximated by $\frac{1}{\Delta t}$, where Δt is the integration time step. In Fig. 16, we compare the expected value of the open-loop surface roughness of Process 3 from the solution of the linearized stochastic KSE model of Eq. (45) to that from a kinetic Monte-Carlo simulation. The two profiles are very close. Therefore, by using the linearized stochastic KSE model of Eq. (45) with the identified model parameters, we can predict the evolution of the expected surface roughness in this sputtering process. This linearized stochastic KSE model is used as the basis for feedback controller design.

4.3.2. Feedback control design

Our control objective is to control the expected surface roughness in Process 3 to a desired value. We design a state feedback controller based on a 40th order stochastic ODE approximation constructed by using the first 40 eigenmodes

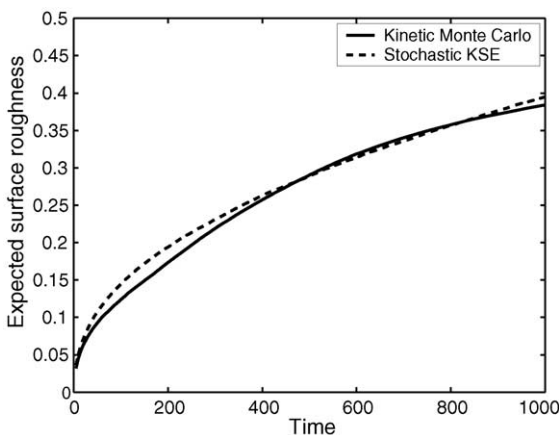


Fig. 16. Comparison of the open-loop profile of the expected surface roughness from the kinetic Monte-Carlo simulator (solid line) and that from the solution of the linearized stochastic Kuramoto-Sivashinsky equation with $\nu = 3.27 \times 10^{-6}$, $\kappa = 1.34 \times 10^{-8}$ and $\sigma = 4.65 \times 10^{-3}$ (dotted line) in Process 3.

of the system of Eq. (47) with identified model parameters $\nu = 3.27 \times 10^{-6}$, $\sigma = 4.65 \times 10^{-3}$ and $\kappa = 1.34 \times 10^{-8}$. Forty control actuators are used to control the system. The i th actuator distribution function is taken to be:

$$b_i(z) = \begin{cases} \frac{1}{\sqrt{\pi}} \sin(iz); & i = 1, \dots, 20 \\ \frac{1}{\sqrt{\pi}} \cos[(i-20)z]; & i = 21, \dots, 40 \end{cases} \quad (55)$$

The desired closed-loop surface roughness is 0.29 in this simulation. Using Eq. (28), we design the state feedback controller such that $\lambda_{c\alpha_i} = \lambda_{c\beta_i} = -0.001$, for $i = 1, \dots, 20$.

Then, we apply the designed controller to the kinetic Monte-Carlo model of Process 3 to control the surface roughness to the desired level. In this simulation, the controller is implemented by manipulating the probability that a randomly selected site is subject to erosion rule, f . Specifically, the f of site i is determined according to the following expression:

$$f(i) = \frac{\bar{f} + (\sum_{j=1}^{40} b_j(z_i) u_j(t))/a}{1 + (\sum_{j=1}^{40} b_j(z_i) u_j(t))/a} \quad (56)$$

The following simulation algorithm is used to run the kinetic Monte-Carlo simulations for the closed-loop system. First, a random number, ζ_1 is generated to pick a site i , among all the sites on the 1D-lattice; the probability that a surface site is subject to the erosion rules, $f(i)$ is determined by using Eq. (56). Then, the second random number, ζ_2 in the $(0, 1)$ interval is generated. If $\zeta_2 < f(i)$, the site i is subject to erosion, otherwise, the site is subject to diffusion.

If the site i is subject to erosion, P_e is computed by using the box rule shown in Fig. 1 with the box centering the surface particle on site i and $Y(\phi_i)$ is computed by using Eq. (1). Then, another random number, ζ_{e3} in the $(0, 1)$ interval is generated. If $\zeta_{e3} < P_e Y(\phi_i)$ the surface particle on site i is removed. Otherwise, no Monte-Carlo event is executed.

If the site i is subject to diffusion, a side-neighbor, $j = i + 1$ or $i - 1$ is randomly picked and the probability of a hopping from site i to site j , $w_{i \rightarrow j}$ is computed based on Eq. (3). Then, another random number ζ_{d3} in the $(0, 1)$ interval is generated. If $\zeta_{d3} < w_{i \rightarrow j}$, the surface particle on site i is moved to site j . Otherwise, no Monte-Carlo event is executed. Once a Monte-Carlo event is executed, the first 40 states ($\alpha_1, \dots, \alpha_{20}$ and $\beta_1, \dots, \beta_{20}$) are updated and new control actions are computed to update the spatially distributed probability that a randomly selected site is subject to erosion rule.

The closed-loop system simulation results are shown in Fig. 17. The dotted line shows the expected surface roughness, which is the average of surface roughness profiles obtained from 200 independent runs, under feedback control. We can see that the controller successfully drives the expected surface roughness to a finite value. The solid line shows the surface roughness profile under feedback control from one simulation run; due to the stochastic nature of the deposition process, stochastic fluctuations can be observed in the closed-loop surface roughness profile, but the surface roughness is

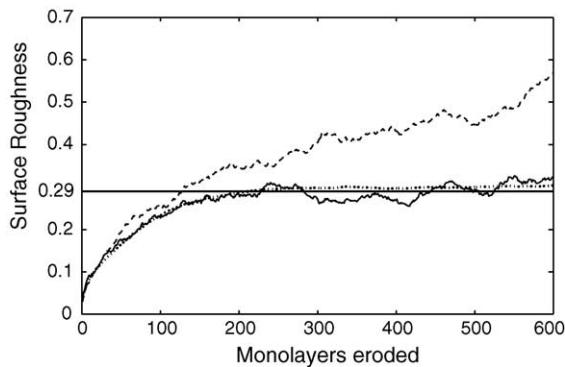


Fig. 17. Closed-loop surface roughness profiles in Process 3. (a) The closed-loop surface roughness profile from one simulation run (solid line); (b) The expected closed-loop surface roughness profile obtained from 200 independent simulation runs (dotted line); and (c) the open-loop surface roughness profile from one simulation run (dashed line).

very close to the expected surface roughness under feedback control. For the sake of comparison, the dashed-line shows a surface roughness profile from one open-loop simulation run. We can see that under feedback control, the surface roughness can be controlled to the desired level.

Remark 7. We note that the proposed methodology can be extended to accommodate unmeasurable process state variables, e.g., it can be extended to perform output feedback control design. In our control problem formulation, the surface roughness control problem is converted to a covariance control problem. Covariance control methods have been developed by Skelton and co-workers in a series of publications, in which, output feedback covariance controllers can be designed by using Kalman filter-based techniques for state reconstruction Hotz and Skelton (1987). Therefore, it is possible to design an output feedback controller based on stochastic PDEs using the developed covariance control theory to control surface roughness.

5. Conclusions

This work focused on control of surface roughness in sputtering processes using the stochastic KSE. We initially reformulated the stochastic KSE into a system of infinite stochastic ordinary differential equations by using modal decomposition. A finite-dimensional approximation of the stochastic KSE was then derived that captures the dominant mode contribution to the surface roughness. A state feedback controller was designed based on the finite-dimensional approximation to control the surface roughness. Feedback control of surface roughness in three different sputtering processes with different sputtering yield functions and different ratios of erosion and diffusion rates was studied. The parameters of the stochastic PDE models describing the sputtering processes were identified by using the surface height fluctuation data obtained from kinetic Monte-Carlo simulations so that

the evolution of the surface roughness computed from the stochastic PDE models is consistent to that computed from kinetic Monte-Carlo simulations. Feedback controllers were designed and applied to kinetic Monte-Carlo models of the sputtering processes. Simulation results demonstrated that the designed feedback controllers can successfully regulate the surface roughness to desired levels.

Acknowledgement

Financial support from the NSF (ITR), CTS-0325246, is gratefully acknowledged.

References

- Åström, K. J. (1970). *Introduction to Stochastic control theory*. New York: Academic Press.
- Armaou, A., & Christofides, P. D. (2000). Feedback control of the Kuramoto–Sivashinsky equation. *Physica D*, 137, 49–61.
- Armaou, A., & Christofides, P. D. (2000). Wave suppression by nonlinear finite-dimensional control. *Chemical Engineering Science*, 55, 2627–2640.
- Armaou, A., Siettos, C. I., & Kevrekidis, I. G. (2004). Time-steppers and ‘coarse’ control of distributed microscopic processes. *International Journal of Robust and Nonlinear Control*, 14, 89–111.
- Chen, L. H., & Chang, H. C. (1986). Nonlinear waves on liquid film surfaces. II. Bifurcation analyses of the long-wave equation. *Chemical Engineering Science*, 41, 2477–2486.
- Chen, Z. Y., Bogaerts, A., Depla, D., & Ignatova, V. (2003). Dynamic Monte Carlo simulation for reactive sputtering of aluminium. *Nuclear Instruments and Methods in Physics Research B*, 207, 415–423.
- Christofides, P. D. (1998). Robust control of parabolic PDE systems. *Chemical Engineering Science*, 53, 2449–2465.
- Christofides, P. D. (2001). *Nonlinear and robust control of PDE systems: Methods and applications to transport-reaction processes*. Boston: Birkhäuser.
- Christofides, P. D., & Armaou, A. (2000). Global stabilization of the Kuramoto–Sivashinsky equation via distributed output feedback control. *Systems & Control Letters*, 39, 283–294.
- Christofides, P. D., & Baker, J. (1999). Robust output feedback control of quasi-linear parabolic PDE systems. *Systems & Control Letters*, 36, 307–316.
- Christofides, P. D., & Daoutidis, P. (1997). Finite-dimensional control of parabolic PDE systems using approximate inertial manifolds. *Journal of Mathematical Analysis and Applications*, 216, 398–420.
- Cuerno, R., & Lauritsen, K. B. (1995). Renormalization-group analysis of a noisy Kuramoto–Sivashinsky equation. *Physical Review E*, 52, 4853–4859.
- Cuerno, R., Makse, H. A., Tomassone, S., Harrington, S. T., & Stanley, H. E. (1995). Stochastic model for surface erosion via ion sputtering: Dynamical evolution from ripple morphology to rough morphology. *Physical Review Letters*, 75, 4464–4467.
- Drotar, J. T., Zhao, Y. P., Lu, T. M., & Wang, G. C. (1999). Numerical analysis of the noisy Kuramoto–Sivashinsky equation in $2 + 1$ dimensions. *Physical Review E*, 59, 177–185.
- Duan, J. Q., & Ervin, V. J. (2001). On the stochastic Kuramoto–Sivashinsky equation. *Nonlinear Analysis*, 44, 205–216.
- Edwards, S. F., & Wilkinson, D. R. (1982). The surface statistics of a granular aggregate. *Proceedings of the Royal Society of London A*, 381, 17–31.

- Fichthorn, K. A., & Weinberg, W. H. (1991). Theoretical foundations of dynamical Monte Carlo simulations. *Journal of Chemical Physics*, 95, 1090–1096.
- Gillespie, D. T. (1976). A general method for numerically simulating the stochastic time evolution of coupled chemical reactions. *Journal of Computational Physics*, 22, 403–434.
- Gilmer, G. H., Huang, H., de la Rubia, T. D., Torre, J. D., & Baumann, F. (2000). Lattice Monte Carlo models of thin film deposition. *Thin Solid Films*, 365, 189–200.
- Haselwander, C., & Vvedensky, D. D. (2002). Fluctuations in the lattice gas for Burgers' equation. *Journal of Physics A: Mathematical and General*, 35, L579–L584.
- Hooper, A. P., & Grimshaw, R. (1985). Nonlinear instability at the interface between two viscous fluids. *Physics Fluids*, 28, 37–45.
- Hotz, A., & Skelton, R. E. (1987). Covariance control theory. *International Journal of Control*, 46, 13–32.
- Insepov, Z., Yamada, I., & Sosnowski, M. (1997). Surface smoothing with energetic cluster beams. *Journal of Vacuum Science & Technology A: Vacuum Surfaces and Films*, 15, 981–984.
- Kalke, M., & Baxter, D. V. (2001). A kinetic Monte Carlo simulation of chemical vapor deposition: Non-monotonic variation of surface roughness with growth temperature. *Surface Science*, 477, 95–101.
- Kardar, M., Parisi, G., & Zhang, Y. C. (1986). Dynamic scaling of growing interfaces. *Physical Review Letters*, 56, 889–892.
- Kersch, A., Morokoff, W., & Werner, C. (1994). Self-consistent simulation of sputter-deposition with the Monte-Carlo method. *Journal of Applied Physics*, 75, 2278–2285.
- Lauritsen, K. B., Cuerno, R., & Makse, H. A. (1996). Noisy Kuramoto-Sivashinsky equation for an erosion model. *Physical Review E*, 54, 3577–3580.
- Liu, W.-J., & Krstić, M. (2001). Stability enhancement by boundary control in the Kuramoto-Sivashinsky equation. *Nonlinear Analysis: Theory, Methods & Applications*, 43, 485–507.
- Lou, Y., & Christofides, P. D. (2003). Estimation and control of surface roughness in thin film growth using kinetic Monte-Carlo models. *Chemical Engineering Science*, 58, 3115–3129.
- Lou, Y., & Christofides, P. D. (2003). Feedback control of growth rate and surface roughness in thin film growth. *A.I.Ch.E. Journal*, 49, 2099–2113.
- Lou, Y., & Christofides, P. D. (2003). Optimal actuator/sensor placement for nonlinear control of the Kuramoto-Sivashinsky equation. *IEEE Transactions on Control Systems Technology*, 11, 737–745.
- Lou, Y., & Christofides, P. D. (2004). Feedback control of surface roughness of GaAs(001) thin films using kinetic Monte-Carlo models. *Computers & Chemical Engineering*, in press.
- Lou, Y., & Christofides, P. D. (2004). Feedback control of surface roughness using stochastic PDEs. *AICHE Journal*, in press.
- Makeev, A. G., Maroudas, D., & Kevrekidis, I. G. (2002a). "Coarse" stability and bifurcation analysis using stochastic simulators: Kinetic Monte Carlo examples. *Journal of Chemical Physics*, 116, 10083–10091.
- Makeev, M. A., Cuerno, R., & Barabasi, A. L. (2002b). Morphology of ion-sputtered surfaces. *Nuclear Instruments and Methods in Physics Research B*, 197, 185–227.
- Ni, D., & Christofides, P. D. (2004). Dynamics and control of thin film microstructure in a complex deposition process. *Chemical Engineering Science*, in press.
- Ni, D., & Christofides, P. D. (2005). Construction of Stochastic PDEs for feedback control of surface roughness in thin film deposition. *International Journal of Robust & Nonlinear Control*, submitted for publication.
- Ni, D., Lou, Y., Christofides, P. D., Sha, L., Lao, S., & Chang, J. P. (2004). Real-time carbon content control for PECVD ZrO_2 thin-film growth. *IEEE Transactions on Semiconductor Manufacturing*, 17, 221–230.
- Palasantzas, G. (1993). Roughness spectrum and surface width of self-affine fractal surfaces via the K -correlation model. *Physical Review B*, 48, 14472–14478.
- Qi, H. J., Huang, L. H., Tang, Z. S., Cheng, C. F., Shao, J. D., & Fan, Z. X. (2003). Roughness evolution of ZrO_2 thin films grown by reactive ion beam sputtering. *Thin Solid Films*, 444, 146–152.
- Reese, J. S., Raimondeau, S., & Vlachos, D. G. (2001). Monte Carlo algorithms for complex surface reaction mechanisms: Efficiency and accuracy. *Journal of Computational Physics*, 173, 302–321.
- Renaud, G., Lazzari, R., Revenant, C., Barbier, A., Noblet, M., Ulrich, O., Leroy, F., Jupille, J., Borensztein, Y., Henry, C. R., Deville, J. P., Scheurer, F., Mane-Mane, J., & Fruchart, O. (2003). Real-time monitoring of growing nanoparticles. *Science*, 300, 1416–1419.
- Schwoebel, R. L. (1969). Step motion on crystal surface II. *Journal of Applied Physics*, 40, 614–618.
- Shitara, T., Vvedensky, D. D., Wilby, M. R., Zhang, J., Neave, J. H., & Joyce, B. A. (1992). Step-density variations and reflection high-energy electron-diffraction intensity oscillations during epitaxial growth on vicinal GaAs(001). *Physical Review B*, 46, 6815–6824.
- Siegert, M., & Plischke, M. (1994). Solid-on-solid models of molecular-beam epitaxy. *Physical Review E*, 50, 917–931.
- Siettos, C. I., Armaou, A., Makeev, A. G., & Kevrekidis, I. G. (2003). Microscopic/stochastic timesteppers and "coarse" control: A kMC example. *AICHE Journal*, 49, 1922–1926.
- Sinha, S. K., Sirota, E. B., Garoff, S., & Stanley, H. B. (1988). X-ray and neutron scattering from rough surfaces. *Physical Review B*, 38, 2297–2311.
- Sivashinsky, G. I. (1977). Nonlinear analysis of hydrodynamic instability in laminar flames. I. Derivation of basic equations. *Acta Astronautica*, 4, 1177–1206.
- Tejedor, P., Šmilauer, P., Roberts, C., & Joyce, B. A. (1999). Surface-morphology evolution during unstable homoepitaxial growth of GaAs(110). *Physical Review B*, 59, 2341–2345.
- Temam, R. (1988). *Infinite-dimensional dynamical systems in mechanics and physics*. New York: Springer-Verlag.
- Van Kampen, N. G. (1992). *Stochastic processes in physics and chemistry*. Amsterdam: North-Holland.
- Villain, J. (1991). Continuum models of crystal growth from atomic beams with and without desorption. *Journal of Physics I*, 1, 19–42.
- Voigtländer, B. (2001). Fundamental processes in Si/Si and Ge/Si studied by scanning tunneling microscopy during growth. *Surface Science Reports*, 43, 127–254.
- Vvedensky, D. D. (2003). Edwards-Wilkinson equation from lattice transition rules. *Physical Review E*, 67, 025102(R).
- Vvedensky, D. D., Zangwill, A., Luse, C. N., & Wilby, M. R. (1993). Stochastic equations of motion for epitaxial growth. *Physical Review E*, 48, 852–862.
- Zapien, J. A., Messier, R., & Collin, R. W. (2001). Ultraviolet-extended real-time spectroscopic ellipsometry for characterization of phase evolution in BN thin films. *Applied Physics Letters*, 78, 1982–1984.
- Ziff, R. M., Gulari, E., & Barshad, Y. (1986). Kinetic phase transitions in an irreversible surface-reaction model. *Physical Review Letters*, 56, 2553–2556.